arXiv:cond-mat/0205416v2 [cond-mat.dis-nn] 22 May 2002

Quantum Collective Creep: a Quasiclassical Langevin Equation Approach

Denis A. Gorokhov[1], Daniel S. Fisher[1], and Gianni Blatter[2]
[1] *Lyman Laboratory of Physics, Harvard University, Cambridge, MA 02138, USA*
[2] *Theoretische Physik, ETH-Hönggerberg, CH-8093 Zürich, Switzerland*

The dynamics of an elastic medium driven through a random medium by a small applied force is investigated in the low-temperature limit where quantum fluctuations dominate. The motion proceeds via tunneling of segments of the manifold through barriers whose size grows with decreasing driving force f. At zero temperature and in the limit of small drive, the average velocity has the form $v \propto \exp[-\text{const.}/\hbar^\alpha f^\mu]$. For strongly dissipative dynamics, there is a wide range of forces where the dissipation dominates and the velocity–force characteristics takes the form $v \propto \exp[-S(f)/\hbar]$, with $S(f) \propto 1/f^{(d+2\zeta)/(2-\zeta)}$ the action for a typical tunneling event, the force dependence being determined by the roughness exponent ζ of the d-dimensional manifold. This result agrees with the one obtained via simple scaling considerations. Surprisingly, for asymptotically low forces or for the case when the massive dynamics is dominant, the resulting quantum creep law is *not* of the usual form with a rate proportional to $\exp[-S(f)/\hbar]$; rather we find $v \propto \exp\{-[S(f)/\hbar]^2\}$ corresponding to $\alpha = 2$ and $\mu = 2(d + 2\zeta - 1)/(2 - \zeta)$, with $\mu/2$ the naive scaling exponent for massive dynamics. Our analysis is based on the quasi-classical Langevin approximation with a noise obeying the quantum fluctuation–dissipation theorem. The many space and time scales involved in the dynamics are treated via a functional renormalization group analysis related to that used previously to treat the classical dynamics of such systems. Various potential difficulties with these approaches to the multi-scale dynamics — both classical and quantum — are raised and questions about the validity of the results are discussed.

I. INTRODUCTION

Static and dynamic properties of elastic systems in the presence of disorder have attracted the attention of physicists for more than three decades. Vortices in superconductors[1], charge density waves in solids[2], domain walls in magnets[3], and geological faults[4] are well-known examples of such systems. Mathematically, some of the problems that arise in modeling are related to those in Burgers turbulence[5], stochastic growth of surfaces[6], and the stability of matter[7]. The physics of dirty elastic systems thus impacts on several disciplines. In this paper we focus on the dynamic properties of driven elastic manifolds at temperatures low enough for quantum fluctuations to play an important role, in particular, the phenomenon of quantum creep.

In many situations the elastic system can be driven by applied forces. For example, transport currents in superconductors cause a Lorentz force to act on vortices, while a magnetic field applied to a ferromagnet produces an effective force on domain walls. One of the primary quantities of interest in such systems is the average velocity v of the manifold as a function of the applied force f, its dependence on the temperature, and on the magnitude of the random disorder that impedes the manifold's motion. The presence of the random pinning forces renders the theoretical analysis difficult, as perturbation theory breaks down in most of the important regimes due to the deformations of the manifold on many length- and time scales. However, some important general results are known: in the absence of thermal and quantum fluctuations the system stays pinned — i.e., the steady state velocity $v = 0$ — if the driving force f is smaller than a certain critical value f_c. At nonzero temperatures, even if the force f is smaller than f_c, the system will move with a nonzero velocity due to thermal creep, see Fig. 1. In the limit $f \ll f_c$ the scaling theory of creep[8–10] predicts the law

$$v \propto \exp\left[-U(f)/T\right], \tag{1}$$

with $U(f) \to \infty$ as $f \to 0$ and there is no linear response to an applied force. The quantity $U(f)$ can be interpreted as a barrier separating two neighboring minima of the free energy on some appropriate length scale that depends on the applied force; on long length- and time scales, the manifold's motion proceeds via thermally activated jumps of corresponding segments between different metastable configurations.

FIG. 1. Tunneling (lower dotted line) and activated motion (upper solid line) of an elastic string in a disordered potential under the action of a weak external force $f \ll f_c$.

Several important assumptions are made in order to derive Eq. (1). First of all, at least in its simplest form, it is assumed that the *barriers* between different metastable configurations scale with length in the same way as the *variations* of the free energy that are caused by the balance between the random pinning and elasticity; in general one could consider two different scaling laws for these quantities[10]. Second, Eq. (1) is an Arrhenius law with *typical* events dominating the creep-like motion. In general, *rare* events, in particular regions with anomalously high barriers, might lead to a modification of this law, perhaps to a form $v \propto \exp\left[-\left(U(f)/T\right)^{\alpha}\right]$ with $\alpha \neq 1$ an exponent characterizing the tails of the barrier probability distribution. Because of these assumptions, as well as the need for increased analytical understanding, it would be valuable to derive the classical creep law (1) starting from a microscopic description. Progress in this direction has recently been made, see Refs. 11,12, where Eq. (1) has been derived from an at-least-partially controllable renormalization group (RG) expansion. Although these results support the validity of the scaling theory for thermal creep, serious questions remain which we will discuss later in this paper. We also note that neither the recent renormalization group calculations nor the present paper address an important aspect of creep in many contexts, in particular in the vortex lattice, i.e., the role of dislocations — the results are, so far, restricted to a truly elastic manifold with pinning weak enough that deformations are too small to induce dislocations or other strongly nonlinear effects[13].

Experimental investigations have shown that even at very low temperatures creep of driven elastic systems, e.g., in vortex lattices[14], of domain walls in magnets[15], and of charge-density waves in solids[16], still persists. This phenomenon suggests an explanation in terms of *quantum tunneling* of the manifold between different metastable configurations; the macroscopic manifestation of this is quantum creep[17]. By analogy with thermal creep, one would guess that

$$v \propto \exp\left[-S(f)/\hbar\right], \tag{2}$$

with $S(f)$ a characteristic action for tunneling of a typical segment of the manifold whose size is determined by the applied force. In spite of a substantial number of studies of quantum creep[14] there is as yet no theoretical analysis that starts from a microscopic description of a driven elastic manifold interacting with impurities; the main goal of this paper is to present a first start at such an analysis, along with a discussion of the difficulties involved. We will show that a law of the form

$$v \propto \exp\left\{-\left[S(f)/\hbar\right]^{\alpha}\right\} \tag{3}$$

can be obtained using a renormalization group approach, as can the functional dependence of the action S on the external force f be found. Whether this is indeed the correct behavior is addressed at the end of the paper.

A natural tool to investigate quantum creep is the functional renormalization group (FRG) expansion[18], an ϵ-expansion near the upper critical dimension ($d_c = 4$) of the random manifold problem. This involves, intrinsically, an infinite number of marginal operators that can be combined into one or more functions. We will find that in this approach a natural separation of the frequency scales occurs between *inter-valley* and *intra-valley* fluctuations of the manifold. The inter-valley fluctuations correspond to the motion of the manifold on large scales on which there are many separate valleys in the "landscape" caused by the randomness. The intra-valley fluctuations correspond to the much faster motion of the manifold within one valley.

The paper is organized as follows. In section II we formulate the model and find the appropriate effective action. In section III we show how to derive the creep law (2) using scaling arguments. Next, we study the problem using the renormalization group expansion (section IV) and then summarize and discuss the main results. We end with an analysis of the limitations and problematic aspects of both our and previous approaches to the creep problem in section V.

II. MODEL AND EFFECTIVE ACTION

We describe the elastic medium by a non-dispersive elastic manifold interacting with a quenched random potential; this generic model captures all the essential physics while allowing for an extensive analytical treatment. The *classical* motion of the displacements $u(\mathbf{z},t)$ of the manifold away from its undeformed state is described by the dynamical equation

$$\eta\partial_t u + \rho\partial_t^2 u = c\nabla^2 u + F(u,\mathbf{z}) + f + f_{\rm th}(\mathbf{z},t), \tag{4}$$

where the friction force $\eta\partial_t u$ and the inertia $\rho\partial_t^2 u$ are balanced by the elastic- ($c\Delta u$), random pinning- ($F(u,\mathbf{z})$), driving- (f), and thermal- ($f_{\rm th}(\mathbf{z},t)$) forces. We will consider the case, applicable to domain walls, of d-dimensional manifolds in $d+1$-dimensional random environments, so that $\mathbf{z}\in\mathcal{R}^d$ and $u\in\mathcal{R}^1$.

The random pinning force $F(u,\mathbf{z})$ is taken to be Gaussian random with mean zero and a correlator

$$\overline{F(u,\mathbf{z})F(u',\mathbf{z}')} = \Delta(u-u')\,\delta(\mathbf{z}-\mathbf{z}'), \tag{5}$$

where the overbar denotes an average over the disorder. The function $\Delta(u)$ decays rapidly with a characteristic scale ξ. The thermal noise $f_{\rm th}(\mathbf{z},t)$ is Gaussian white with a correlator

$$\langle f_{\rm th}(\mathbf{z},t) f_{\rm th}(\mathbf{z}',t')\rangle = 2\eta T\,\delta(t-t')\delta(\mathbf{z}-\mathbf{z}') \equiv \kappa(t-t')\,\delta(\mathbf{z}-\mathbf{z}'), \tag{6}$$

with $\langle\ldots\rangle$ denoting the average over thermal fluctuations.

In classical statistical mechanics we can reformulate the problem posed by a stochastic differential equation as an effective field theory[19,20] with the help of the Martin-Siggia-Rose (MSR) approach. After averaging over thermal fluctuations the MSR-action corresponding to (4) has the form

$$\begin{aligned} A_{\rm MSR} = &-\int d^d z dt\, iy(\mathbf{z},t)\big(\eta\partial_t u + \rho\partial_t^2 u - c\Delta u\big) \\ &+ \int d^d z dt\, iy\big(f + F(u,\mathbf{z})\big) \\ &+ \frac{1}{2}\int d^d z dt dt'\, iy(\mathbf{z},t)\kappa(t-t')iy(\mathbf{z},t'), \end{aligned} \tag{7}$$

with $y(\mathbf{z},t)$ an auxiliary field used to enforce the equation of motion. The probability of a particular dynamical evolution $\bar{u}(\mathbf{z},t)$ under the stochastic process is proportional to $\int\mathcal{D}[y]\,\exp\{A_{\rm MSR}[\bar{u},y]\}$.

The main goal of this paper is to investigate the influence of quantum fluctuations on the system whose *classical limit* is described by Eq. (4). Again, it is convenient to formulate the problem as a field-theory, i.e., to write the effective action describing the elastic system in the presence of quantum fluctuations in a way analogous to (7). When calculating time-independent quantities in equilibrium systems (i.e., in the case $f=0$) the corresponding quantum action has a Euclidean form and the quantum partition function can be written as an imaginary time path integral[21]. However, here we are interested in non-equilibrium properties ($f\neq 0$) and the Euclidean action cannot be used.

A formalism allowing to study the *real time* dissipative quantum mechanics of a system is that of Feynman and Vernon[22]: the quantum amplitude $\Psi(x_f,t_f;x_i,t_i)$ for a system to have a coordinate x_f at time t_f, if at time t_i it had a coordinate x_i, can be written as a path integral $\int_{x_i,t_i}^{x_f,t_f}\mathcal{D}[x]\exp(iS[x]/\hbar)$, with $S[x]$ the classical action. Consequently, the probability of the transition $x_i,t_i\to x_f,t_f$ can be written in the form

$$\mathcal{P}(x_f,t_f;x_i,t_i) = \int_{x_i,t_i}^{x_f,t_f}\int_{x_i,t_i}^{x_f,t_f}\mathcal{D}[x]\mathcal{D}[x']\exp(iS[x]/\hbar)\exp(-iS[x']/\hbar). \tag{8}$$

In non-equilibrium quantum mechanics the functional (8) plays the same role as the partition function in equilibrium problems. We see that the effective action can be written as $iS[x]-iS[x']$ and includes two different paths $[x(t)]$ and $[x'(t')]$.

The standard way to include dissipation is to write the action $S[x]$ in the form $S[x]=S_0[u]+S_{\rm bath}[X_{\rm bath}]+S_{\rm int}[x]$ representing the actions corresponding to the elastic manifold, the bath, and the interaction between the bath and the manifold, respectively (note that $x=(u,X_{\rm bath})$ and $x'=(u',X'_{\rm bath})$ are the coordinates describing both the manifold and the bath). In the Caldeira-Leggett model[23] the terms $S_{\rm bath}[X_{\rm bath}]$ and $S_{\rm int}[x]$ are taken to be quadratic in the bath coordinate $X_{\rm bath}$ and hence can be integrated out at the expense of effective interactions that couple different times. The resulting action takes the form (see appendix A or Ref. 24)

$$\frac{iS[\tilde{u},\tilde{y}]}{\hbar} = -\frac{i}{\hbar}\int d^d z dt\, \tilde{y}(\mathbf{z},t)\left(\eta\partial_t\tilde{u} + \rho\partial_t^2\tilde{u} - c\Delta\tilde{u}\right) + \frac{1}{2\hbar^2}\int d^d z dt dt'\, i\tilde{y}(\mathbf{z},t)\kappa(t-t')i\tilde{y}(\mathbf{z},t') - \frac{i}{\hbar}\int d^d z dt\Big[U(\tilde{u}+\frac{\tilde{y}}{2},\mathbf{z}) - U(\tilde{u}-\frac{\tilde{y}}{2},\mathbf{z}) - f\tilde{y}\Big], \tag{9}$$

with

$$\tilde{u}(\mathbf{z},t) = (u(\mathbf{z},t) + u'(\mathbf{z},t))/2,$$
$$\tilde{y}(\mathbf{z},t) = u(\mathbf{z},t) - u'(\mathbf{z},t),$$

and the random potential

$$U(u,\mathbf{z}) = -\int^u du_1 F(u_1,\mathbf{z}).$$

The Fourier transform of the effective noise correlator $\kappa(t-t')$ of the bath fluctuations obeys the quantum fluctuation–dissipation theorem,

$$\kappa(\omega) = \eta\hbar\omega\coth\frac{\hbar\omega}{2T}, \tag{10}$$

where η is related to the spectral density of the bath, see appendix A.

The action (9) allows one, in principle, to investigate all the properties of a driven elastic medium in the presence of quantum fluctuations. The classical limit, the MSR action $A_{\rm MSR} = iS/\hbar$ can be recovered by expanding the random potential energy U in the $\tilde{y}$-field and substituting $\tilde{u}$ by u and $\tilde{y}/\hbar$ by y. Such an expansion is valid at high temperatures and it has been argued[25] that it also applies to the limit $\hbar \to 0$ at $T = 0$. This suggests that the dynamics of quantum systems in the semiclassical regime, where tunneling processes through large barriers dominate, can be described by Eq. (4) with the noise obeying the fluctuation–dissipation theorem (10); this is called the quasi-classical Langevin equation[25] (QLE) approach. In a number of papers[26,27] the QLE has been used to study the non-equilibrium dynamics of quantum systems. In particular, in Ref. 26 the quantum tunneling of an overdamped quantum particle has been studied using this approximation. Writing the inverse lifetime Γ of a metastable state in the form $\Gamma = Pe^{-S/\hbar}$ with S the tunneling action and P the prefactor, it turns out[26], that the QLE gives the correct value of the tunneling action S up to a multiplicative factor of order unity (note that for quadratic systems the QLE is actually *exact*, as is the expansion $U(\tilde{u}+\tilde{y}/2,\mathbf{z}) - U(\tilde{u}-\tilde{y}/2,\mathbf{z}) \approx U'(\tilde{u},\mathbf{z})\,\tilde{y}$ for this case).

In this paper we use the QLE to study quantum creep in a disordered medium. Although we would like to do better, we are primarily interested in obtaining the correct *scaling* laws and asymptotic forms; the exact coefficients are of less interest. The action (7) with the quantum noise (10) is much simpler to analyze than the full quantum action (9). We believe that the QLE should be a useful tool for investigating the dynamics of quantum systems as it appears to capture the essential physics, while being — at least relatively — tractable analytically. Quantum fluctuations appear in the QLE approach as an effective random force with a correlator $\kappa(t)$, see (10), acting on the system. The quantum decay of a metastable state then is equivalent to the thermally activated escape of a particle driven by colored noise[28].

III. SCALING ARGUMENTS

A. Statics and Thermal Creep

An elastic manifold subject to a random potential behaves as an assembly of approximately independently pinned segments of a characteristic size that is determined by the balance between the pinning and elastic forces. The driven motion of the manifold is dominated, both classically and quantum mechanically, by successive jumps of segments of the manifold between subsequent metastable configurations. In order to understand this behavior one needs to consider various characteristic scales.

The characteristic size of the collectively pinned segments is of order[1] $L_c \sim [c^2\xi^2/\Delta(0)]^{1/(4-d)}$, the Larkin length over which the typical distortion of the manifold $|u(L_c) - u(0)|$ is of order ξ, the scale of the correlations in the random pinning landscape. The characteristic energy scale of the deformations on scale L_c is $U_c \sim c\xi^2 L_c^{d-2}$. Beyond

L_c, the typical displacements of the manifold grow as $|u(L) - u(0)| \sim \xi(L/L_c)^\zeta$ with ζ the wandering exponent, $\zeta = (4-d)/3$ for the random force case, while $\zeta_{d,1} \approx 0.2083\,(4-d)$ for a short-range correlated random potential; the difference in energy between metastable configurations deviating on a scale L by a displacement $\delta u(L)$ is controlled by the balance between the elastic- and pinning energies, both of which have a magnitude of order $U_c(L/L_c)^\theta$ with the energy exponent $\theta = d + 2\zeta - 2$ and the wandering exponent ζ given above.

In the presence of an applied force f it is favorable for a segment of size L to move into the neighboring metastable valley if the energy $fL^d\delta u(L) \sim fL^d\xi(L/L_c)^\zeta$ gained due to the presence of the force is larger than the difference of the elastic- plus pinning energies between the two configurations; for small forces, this will only occur for large segments. Equating the two energy scales, we obtain the minimum characteristic size of a segment that can move to the lower energy site[8],

$$L_f \sim L_c\left(\frac{f_c}{f}\right)^{1/(2-\zeta)}, \tag{11}$$

where $f_c \sim c\xi/L_c^2$ is the critical applied force needed to move the manifold in the absence of thermal or quantum fluctuations. The scale L_f is the minimum size of a segment that can hop in order to lower its energy; the macroscopic motion then proceeds via jumps of segments of this characteristic size over distances

$$u_f \sim \xi\left(\frac{f_c}{f}\right)^{\zeta/(2-\zeta)} \tag{12}$$

separating two neighboring metastable configurations.

Consider first the classical motion, i.e., thermal creep: The conventional assumption is that the height of the energy barrier that must be surmounted for such a motion to occur classically is determined by the scaling of the *static* energy $U_c(L/L_c)^\theta$ (we will discuss the validity of this assumption later in this section). The characteristic height of the barrier that dominates the motion at a small force f then is

$$U(f) \sim cu_f^2 L_f^{d-2} \sim U_c(L_f/L_c)^{d+2\zeta-2} \sim U_c(f_c/f)^{(d+2\zeta-2)/(2-\zeta)}; \tag{13}$$

this yields an average velocity for thermal creep, see Ref. 8,

$$v \sim \exp[-U(f)/T]. \tag{14}$$

B. Quantum Creep with Dissipative Dynamics

The quantum tunneling of segments of the manifold can be estimated in a manner analogous to their classical thermal activation: Let us assume that the manifold is located in one of the metastable configurations and subject to a small driving force f. One expects the lifetime of such a state to be proportional to $\exp(S/\hbar)$, with S the characteristic action describing the tunneling through the barrier separating the metastable minimum from one with a lower energy. We estimate S using the standard theory of the decay of metastable states. We first assume that the effects of dissipation dominate over those of inertia; the Euclidean action of the manifold then can be written in the form

$$S_{\rm Eucl}[u] = \int_{-\infty}^{+\infty} d\tau \int d^d z \left[\frac{c}{2}\left(\frac{\partial u}{\partial \mathbf{z}}\right)^2 + U(u,\mathbf{z}) - fu + \frac{\eta}{4\pi}\int_{-\infty}^{+\infty} d\tau' \frac{(u(\mathbf{z},\tau) - u(\mathbf{z},\tau'))^2}{(\tau-\tau')^2}\right], \tag{15}$$

with τ the imaginary time and η the dissipative coefficient. In order to find S one needs to find the imaginary time trajectory connecting the initial and final configurations of the manifold and calculate its action. We emphasize that as our problem is a non-equilibrium one, the full quantum action (9) should be used. However, at low driving forces, the problem we study is a *quasi-stationary* one, as the lifetime of a metastable state is large and the manifold can be considered to be in local equilibrium. Therefore we can use the simpler (Euclidean) action (15) instead of the full dynamic action (9).

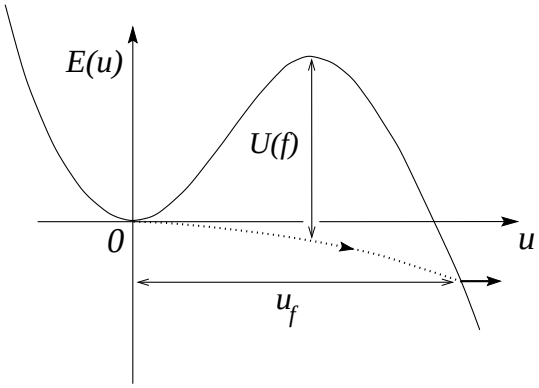

FIG. 2. Tunneling of a particle with an effective mass ρL_f^d and dissipative coefficient ηL_f^d through a barrier of height $U(f)$ and width L_f.

In estimating the tunneling action we find the size L_f of the tunneling segment as in the classical case of thermal creep, since this is determined by the *static* balance between the variations in the pinning energy and the energy gain due to the external force. Furthermore, we assume that there is only one characteristic time scale τ_f associated with the tunneling process. We can then consider the tunneling event, crudely, as an effective process in which a point-like object with a friction coefficient $\eta_f = \eta L_f^d$ tunnels through a potential barrier of height $U(f)$ and extent u_f, see Fig. 2. The saddle-point of the action (15) is minimized when

$$\eta_f \frac{u_f}{\tau_f} \sim \frac{U(f)}{u_f}, \tag{16}$$

where we have substituted the dynamic term by its characteristic value and $U(f)/u_f$ is the characteristic force acting on the "particle". The tunneling time τ_f is given by $\tau_f \sim \eta_f u_f^2/U(f)$, resulting in the tunneling action

$$S(f) \sim S_\eta \left(\frac{f_c}{f}\right)^{(d+2\zeta)/(2-\zeta)}, \tag{17}$$

with $S_\eta \sim \eta \xi^2 L_c^d$ the characteristic scale of the dissipative action of a segment with the diameter of the order of the Larkin length L_c. The velocity of the manifold is related to $S(f)$ via (2).

The characteristic crossover temperature $T_{\rm cr}$ from quantum to classical creep can be obtained by comparing $U(f)/T$ and $S(f)/\hbar$, i.e.,

$$T_{cr} \sim \frac{\hbar U(f)}{S(f)} \sim \frac{\hbar U_c}{S_\eta}\left(\frac{f}{f_c}\right)^{2/(2-\zeta)} \tag{18}$$

gives the scaling conjecture for the dissipative limit.

C. Quantum Creep with Inertial Dynamics

We now assume that the inertial term in the action is more important for the tunneling process than the dissipation. In this case the Euclidean action analogous to that given by (15) can be written in the form

$$S_{\rm Eucl}[u] = \int_{-\infty}^{+\infty} d\tau \int d^d z \left[\frac{c}{2}\left(\frac{\partial u}{\partial \mathbf{z}}\right)^2 + U(u,\mathbf{z}) - fu + \frac{\rho}{2}\left(\frac{\partial u}{\partial t}\right)^2\right], \tag{19}$$

with ρ the mass density of the manifold. The size L_f of the tunneling segment is the same as in the dissipative case. In order to find the action $S(f)$ one again needs to find the tunneling time τ_f; comparing kinetic and pinning energies for the saddle-point configuration, we find (with $\rho_f = \rho L_f^d$ the effective mass of the tunneling object)

$$\rho_f \frac{u_f}{\tau_f^2} \sim \frac{U(f)}{u_f}, \tag{20}$$

i.e., $\tau_f \sim [\rho_f/U(f)]^{1/2} u_f$, and the tunneling action can be estimated as

$$S(f) \sim S_\rho \left(\frac{f_c}{f}\right)^{(d+2\zeta-1)/(2-\zeta)}, \tag{21}$$

with $S_\rho \sim (\rho U_c L_c^d)^{1/2}\xi$ the characteristic action with inertial dynamics on the Larkin scale L_c. The quantities L_c and U_c have been defined in section III A above. The characteristic crossover temperature can be determined as in the dissipative case and is given by $T_{cr} \sim (\hbar U_c/S_\rho)(f/f_c)^{1/(2-\zeta)}$.

D. Assumptions

Two important assumptions have been made in order to derive the scaling prediction (2): First of all, it has been assumed that the barriers for the manifold's motion scale in the same way as the variations of the energy. If there are two independent exponents $\theta = d-2+2\zeta$ parametrizing the *static* energy scaling and $\psi > \theta$ characterizing the scaling of energy barriers[29,30], then the barrier for thermal creep will have the form $U(f) \propto L_f^\psi$. The simplest assumption for the quantum motion is that this same barrier height is the appropriate one for the quantum barrier traversal. While the dissipative result (17) would remain the same (as $S_{\rm diss} \sim \eta_f u_f^2$ does not depend on the height of the tunneling barrier), the result for the inertial dynamics would take the form $S_{\rm inertial} \propto L_f^{(d+\psi+2\zeta)/2}$.

We should emphasize, however, that if $\psi > \theta$ then this is because the dynamics on intermediate length scales affects that on the large scale L_f. A dependence of the large scale dynamics, of interest for quantum creep at small applied forces, on the intermediate scale physics can also occur quantum mechanically; but the way in which it occurs could be quite different from the classical situation and it is possible that each type of quantum dynamics has its own exponent ψ_Q distinct from the classical value ψ[31]. Once we admit the possibility of a dependence of the tunneling dynamics of large segments on the dynamics at intermediate scales, the basic assumptions of the scaling arguments given above break down. But this is exactly the kind of problem for which a renormalization group framework is needed.

Another potentially important effect that was not taken into account in the simple scaling analysis summarized above are rare events: in general, it is possible that the velocity is not controlled by the typical barriers — or, more precisely, by the tunneling through these typical barriers — but by rare anomalously large barriers. In the simplest scenario, this could give rise to a quantum creep law of the form $v \propto \exp\{-[S(f)/\hbar]^\alpha\}$, with $\alpha \neq 1$ a non-trivial exponent characterizing the tail of the distribution of barrier heights. Just such a phenomenon controls the temperature dependence of the diffusion coefficient of a single particle diffusing in a Gaussian random potential[32], see the discussion in section IV E. One mechanism for an exponent $\alpha > 1$ is that rare, rather than typical, events dominate the macroscopic motion.

IV. RENORMALIZATION GROUP ANALYSIS

A. Derivation of RG Equations

Having presented the basic scaling arguments for both classical and quantum creep, we now turn to the main task of this paper, an attempt to derive the creep laws from a microscopic description of the dynamics. With the roughness exponent ζ vanishing in dimensions $d > 4$, one expects that $d_c = 4$ is the upper critical dimension of randomly pinned elastic manifolds, an expectation which turns out to be correct both for the equilibrium properties in the absence of a driving force and for the fluctuationless ($T = 0$) critical depinning transition at f_c in the presence of a driving force f. A renormalization group ϵ-expansion about $d_c = 4$ then allows one to investigate the various large scale properties of the pinned elastic manifold[18]. An important feature of this renormalization group analysis is the fact that even to lowest order one has to take into account infinitely many variables, in practice by renormalizing a function that is essentially the correlator $\Delta[u(\mathbf{z}) - u(\mathbf{z}')]$ of the random force (but see the discussion in Ref. 33 and in section V B).

The functional renormalization group (FRG) approach has been successfully applied to both static equilibrium[18] and fluctuationless ($T = 0$) depinning problems[34,35]. Recently, the FRG has also been applied to the thermal creep problem[11,12,36], although its applicability is far more problematic. For forces $f \ll f_c$, the motion proceeds either by activation or tunneling of large segments between different metastable minima and thus the dynamics is *intrinsically* non-perturbative: in particular, the dynamic exponent z, which is shifted only slightly from its naive value of two near the critical depinning transition, must be radically modified in the creep regime. Nevertheless, it *appears* (though, see section V) that for thermal depinning one can handle this within the FRG and renormalize until a scale is reached

beyond which the disorder can be taken into account perturbatively and the equation of motion can be solved. By retracing back the FRG flow, one can then determine the average velocity of the manifold. We will follow this approach here, but return later in the paper to question its validity both for the quantum and classical cases.

Formally, in both classical and quantum cases, the RG analysis of creep involves the flow away from the static ($f = 0$) fixed-point that controls the undriven pinned system under the action of a small applied force f; under the RG transformation the parameters describing the system flow in such a way that eventually the effects of disorder can be neglected beyond a certain length scale. But there is an important difference between the classical and quantum cases: In the classical case[12] one can restrict the analysis to the low-frequency limit, i.e., including the friction term ($\eta\partial_t u$) alone into the renormalization procedure is sufficient. This is a consequence of the fact that, to exponential accuracy, classical creep does not depend on the dynamics (e.g., inertial versus dissipative) of the system. In the quantum case, it will turn out that an analogous treatment leads to a spurious "localization transition" where the average velocity of the manifold drops to zero at a finite length scale $\sim L_c$, see section IV B. In order to carry out a correct analysis one must include *all* the frequencies into the renormalization group; specifically, we must make the substitution

$$\eta\partial_t u \to \hat{D}\otimes u \equiv \int_{-\infty}^{t} d\tau D(\tau)u(t-\tau) \equiv \eta\partial_t u + \sum_{k=2}^{\infty}\eta^{(k)}\partial_t^k u. \tag{22}$$

It will turn out that, even if initially $\eta^{(k)} \equiv 0$ for all $k \geq 2$, the dynamic parameters $\eta^{(k)}$ will grow rapidly under the flow and become crucial; the renormalized spectrum $D_l(\omega)$ is very different from the bare linear spectrum $-i\omega\eta$.

It has been argued above that in order to investigate quantum creep we can use the action (7) with the correlator given by (10). It is convenient to perform the disorder average in (7) and work in a frame moving at the average velocity of the manifold, i.e., we substitute $u(\mathbf{z},t) \to u(\mathbf{z},t) + vt$. We also introduce the above general dynamics $\hat{D}$; the resulting action, averaged over both quantum fluctuations and random pinning, takes the form

$$\begin{aligned} A = &-\int d^d z dt\, iy\big(\hat{D}\otimes u - c\partial_{\mathbf{z}}^2 u\big) + \frac{1}{2}\int d^d z dt dt'\, iy(\mathbf{z},t)\kappa(t-t')iy(\mathbf{z},t') \\ &+ \int d^d z dt\, iy\,(f-\eta v) + \frac{1}{2}\int d^d z dt dt'\, iy(\mathbf{z},t)\Delta\big[u(\mathbf{z},t) - u(\mathbf{z},t') + v(t-t')\big]iy(\mathbf{z},t'). \end{aligned} \tag{23}$$

The correlation functions corresponding to the quadratic action in the absence of pinning are given by

$$\overline{u(\mathbf{k},\omega)u(\mathbf{k}',\omega')} = \frac{\kappa(\omega)}{|c\mathbf{k}^2 + D(\omega)|^2}\delta(\omega+\omega')\delta(\mathbf{k}+\mathbf{k}') \equiv C(\mathbf{k},\omega)\delta(\omega+\omega')\delta(\mathbf{k}+\mathbf{k}'), \tag{24}$$

$$\overline{u(\mathbf{k},\omega)iy(\mathbf{k}',\omega')} = \frac{1}{c\mathbf{k}^2 + D(\omega)}\delta(\omega+\omega')\delta(\mathbf{k}+\mathbf{k}') \equiv R(\mathbf{k},\omega)\delta(\omega+\omega')\delta(\mathbf{k}+\mathbf{k}'), \tag{25}$$

with the usual definition of the Fourier transform

$$f(\mathbf{k},\omega) \equiv \int d^d z dt\, f(\mathbf{z},t)\exp\left(-i\mathbf{k}\mathbf{z} + i\omega t\right) \tag{26}$$

and $D(\omega) \approx \eta(-i\omega)$ for small ω. Because of the fluctuation dissipation theorem, we have

$$\kappa(\omega) = -\hbar\,\mathrm{Im}D(\omega)\,\coth\frac{\hbar\omega}{2T}. \tag{27}$$

In the regime of interest for quantum creep, the motion of the elastic manifold can be represented as jumps between different metastable states and the lifetime of each metastable state is large. It is thus possible to extract some information about the dynamic properties of the system, in particular, the average velocity v, from *static* equations if we cutoff the renormalization group flow at the relevant length scale, here, $L_f \sim L_c(f_c/f)^{1/(2-\zeta)}$, see section III (a similar situation arises in the conventional theory of the decay of metastable states: although the original problem is formally non-equilibrium, the system is trapped for a long time in the local equilibrium state corresponding to a local minimum of the free energy; one can approximate the partition function of the system by that calculated assuming quasi-equilibrium and then find the flow of the probability out of the local potential well). This is why we could use the Euclidean action instead of the full quantum mechanical action in section III. For values of the RG variable l smaller than $\ln(L_f/L_c)$ we then can use the appropriate static versions of RG equations.

The RG flow equations are obtained by integrating over fast modes in the effective action (23) with the last two terms in the action treated as perturbations about the quadratic action. We write all the equations, except those for

the correlator $\Delta_l(u)$, the temperature T_l, and the Planck constant $\hbar_l$, at finite velocity. We will use the subscript l in order to distinguish renormalized quantities at length scale $L = \Lambda^{-1}e^l$ from bare quantities without subscripts, e.g., $\eta = \eta_0$, $T = T_0$, $\hbar = \hbar_0$, $\Delta(u) = \Delta_0(u)$, etc. Introducing the large momentum cutoff Λ we obtain to leading non-trivial order in Δ_l,

$$\begin{aligned}
\partial_l \Delta_l(u) &= (4-d-2\zeta)\,\Delta_l(u) + \zeta u \Delta_l'(u) + C_l^>(\Lambda, t=0)\Delta_l''(u) \\
&\quad + I\Delta_l''(u)\big[\Delta_l(0) - \Delta_l(u)\big] - I\Delta_l'^2(u), && (28)\\
\partial_l \tilde{f}_l &= (2-2\zeta)\tilde{f}_l + \int dt R_l^>(\Lambda,t)\Delta_l'(v_l t), && (29)\\
\partial_l v_l &= (z-\zeta)\, v_l, && (30)\\
\partial_l \kappa_l(t) &= (4-d-2\zeta)\kappa_l(t) + zt\partial_t\kappa_l(t) - C_l^>(\Lambda,t)\Delta_l''(v_l t), && (31)\\
\partial_l D_l(\omega) &= 2D_l(\omega) - z\omega\partial_\omega D_l(\omega) - \int \frac{d\omega'}{2\pi}\frac{1}{v_l}\hat{\Delta}_l''(\omega'/v_l)\left[R_l^>(\Lambda,\omega') - R_l^>(\Lambda,\omega+\omega')\right], && (32)\\
\partial_l T_l &= (2-d-2\zeta)\, T_l, && (33)\\
\partial_l \hbar_l &= (2-d-2\zeta-z)\,\hbar_l, && (34)
\end{aligned}$$

with $I \equiv A_d\Lambda^d/c^2\Lambda^4$ defined in terms of the surface area A_d of a d-dimensional unit sphere. Both the dynamic exponent $z = z(l)$ and the roughness exponent $\zeta(l)$ are at our disposal to adjust for convenience; it will generally be most useful to choose ζ to be the l-independent value giving rise to a well behaved fixed point function $\Delta^*(u)$ in the absence of fluctuations or drive. How best to adjust $z(l)$ we reserve for later; conventionally it would be chosen to fix the coefficient in the low-frequency part of $D_l(\omega)$, in the dissipative situation studied here, of η_l. The shell-restricted correlation functions $C^>(\Lambda,t)$ and $R^>(\Lambda,t)$ are given by

$$C_l^>(\Lambda,t) = \frac{A_d\Lambda^d}{(2\pi)^d}\int \frac{d\omega}{2\pi} e^{-i\omega t} C(\Lambda,\omega) \tag{35}$$

and

$$R_l^>(\Lambda,t) = \frac{A_d\Lambda^d}{(2\pi)^d}\int \frac{d\omega}{2\pi} e^{-i\omega t} R(\Lambda,\omega); \tag{36}$$

here, $C(\Lambda,\omega)$ and $R(\Lambda,\omega)$ are defined via (24) and (25) with $D(\omega)$ substituted by $D_l(\omega)$. Also, we define the coefficient

$$\Gamma_l \equiv C_l^>(\Lambda, t=0), \tag{37}$$

which will appear frequently in the following. We chose an initial dynamic spectrum of the form

$$D_0(\omega) = -i\eta\omega + \rho\omega^2. \tag{38}$$

The excess of the applied force over that needed to sustain the motion of an unpinned system with dissipative coefficient η_l is

$$\tilde{f}_l = f_l - \eta_l v_l. \tag{39}$$

Above, we have defined the Fourier transform of the second derivative $\Delta''(u) \equiv \partial_u^2\Delta$ by $\hat{\Delta}''(p) \equiv \int du\, e^{ipu}\Delta''(u)$, so that

$$\hat{\Delta}_l''(\omega/v) \equiv v\int_{-\infty}^{+\infty} dt e^{i\omega t}\Delta_l''(vt); \tag{40}$$

this quantity plays a crucial role in the dynamic renormalization. Eqs. (28), (29), (31), (30), and (33) have been obtained before in the discussion of classical creep[12]; they are the same in the quantum case, while Eq. (32) is different, however. We now show how it can be obtained and in what respect it differs from its classical analog.

After averaging the disorder term over the fast modes one obtains the following feedback δA to the term $-\int d^dz dt\, iy(\mathbf{z},t)\tilde{D}_l \otimes u$ in the action,

$$\delta A = -\int d^Dz dt dt'\, iy(\mathbf{z},t) R_l^>\,(\Lambda, t-t')\,[u(\mathbf{z},t) - u(\mathbf{z},t')]\,\Delta_l''\,[v(t-t')]\,dl. \tag{41}$$

Writing the functions $\Delta_l(v\tau)$ and $R_l^>(\Lambda,\tau)$ as Fourier integrals we obtain Eq. (32), which explicitly includes the full dependence of the displacement field $u(\mathbf{z},t)$ on time, i.e., it is nonperturbative in frequency. In the classical analysis of Ref. 12 it was assumed that the low-frequency limit of the RG equations is valid for all frequencies, i.e., for $\omega \to 0$ the only important term is that containing $\eta_l \partial_t u$ (corresponding to $-\eta_l i\omega u(\omega)$ in Fourier space). The equation analogous to (32) then is given by its low-frequency limit, i.e., instead of the full dependence $u(\mathbf{z},t) - u(\mathbf{z},t')$ one considers only the first term of its Taylor expansion in $t - t'$. It was also assumed in Ref. 12 that the response function $R_l^>(\Lambda,t)$ and the correlation function $C_l^>(\Lambda,t)$ depend only on the frictional coefficient η_l. In the classical limit this approach leads to reasonable results. By contrast, ignoring the frequency dependence of the dynamics in the quantum case leads to a spurious "localization transition", implying a zero average velocity of the manifold below a small but non-zero driving force f and in the presence of quantum fluctuations $\hbar \neq 0$. We will discuss this issue in section IV B.

In the case of a purely dissipative dynamics there is another problem that occurs even at the initial stage of the renormalization: the integral in the expression for $C_l^>(\Lambda, t=0)$ diverges at large frequencies, see Eqs. (35) and (24). For large ω the noise $\kappa_l(\omega)$ (see (10)) and the dynamic spectrum $D_l(\omega)$ are both proportional to ω for a dissipative dynamics and, consequently, $C_l^>(\Lambda, t=0)$ diverges logarithmically as $\int d\omega/\omega$ at large frequencies, see (24). This is not unexpected: it is just such a logarithmic frequency dependence that can cause localization in models with a single degree of freedom coupled to a bath that provides a linear friction[37]; thus integrating out all the frequencies at once is problematic even for short wavelength deformations of the manifold. In reality, we expect that an inertial term $\rho\partial_t^2 u$ or some other frequency dependence describing the small scale dynamics will provide a cutoff at high frequencies (at $\omega_0 \sim \eta/\rho$ for the inertial case); alternatively one could introduce a sharp cutoff by hand. We will consider both possibilities later, noting now that how this is done will affect the results far more than one might expect.

B. Structure of the Quantum RG Flow

The main goal of the remainder of this section is to analyze the system of RG equations derived in section IV A in the limit of small driving forces. We first discuss the important features and then provide a more detailed analysis in the following section. First, let us analyze the renormalization (28) of the force-force correlator. In the absence of quantum and thermal fluctuations (i.e., $\kappa(\omega) = 0$ for all ω), the correlation function $C_l^>(\Lambda, t=0)$ is zero. In this case, the nonlinearities in the flow equation of the function $\Delta_l(u)$ cause it to become nonanalytic on a finite length scale, even if the bare correlator $\Delta_0(u)$ is analytic, see Ref. 18. This is easily seen by differentiating Eq. (28) twice with respect to u and substituting $u = 0$, resulting in an equation for the evolution of the quantity $\Delta_l''(0)$ alone. The simple autonomous flow equation for $\Delta_l''(0)$ leads to a divergence at a finite scale $l_c \sim \epsilon^{-1} \ln[c^2/\Lambda^{d-4}\Delta_0''(0)]$, producing the Larkin- or pinning length $L_c \simeq [c^2/\Delta''(0)]^{1/(4-d)} \sim [c^2\xi^2/\Delta(0)]^{1/(4-d)}$ where collective pinning goes over into strong pinning. Beyond L_c, the perturbative description breaks down as multiple competing minima appear in the pinning energy landscape. The infinite second derivative suggests that the function $\Delta_l(u)$ will have a discontinuous first derivative at $u = 0$, i.e., $\Delta_l'(+0) = -\Delta_l'(-0) \neq 0$. On length scales shorter that L_c, the smoothness of $\Delta_l(u)$ reflects the smooth reversible evolution of a segment as it is pulled by its neighboring regions. But on larger length scales the internal deformations of the segment will cause it to jump discontinuously and irreversibly from one metastable configuration to another — this is reflected in the discontinuity in Δ_l'. At the scale L_c the force correlator essentially has reached its fixed point shape with a height $\Delta^*(0) \sim (c\Lambda^2)^2\xi^2\Lambda^{-d}e^{-2\zeta l_c}$ and a width $\xi^* \sim \xi e^{-\zeta l_c}$, resulting in a cusp $|\Delta^{*\prime}(0+)| \sim (c\Lambda^2)^2\xi\Lambda^{-d}e^{-\zeta l_c}$, see appendix B.

In the presence of small quantum or thermal fluctuations the coefficient $\Gamma_l \equiv C_l^>(\Lambda, t=0)$ becomes nonzero and this leads to a *smearing* of the cusp in $\Delta_l(u)$[11,12,38]. The derivative $\Delta_l'(0)$ of the correlator at the origin is zero for $C^>(\Lambda, t=0) \neq 0$ but changes rapidly in a boundary layer around the origin. The cusp that was present in the absence of fluctuations is smeared over a region $u_{\rm smear}$ which can be estimated by comparing[12] the terms $\Gamma_l\,|\Delta_l''(0)| \sim \Gamma_l\,|\Delta_l'(u \sim u_{\rm smear})|\,/u_{\rm smear}$ and $[\Lambda^d/(c\Lambda^2)^2]\Delta_l'^2(u)$ in (28). The derivative $\Delta_l'(u > u_{\rm smear})$ approaches the fixed point value $\Delta^{*\prime}(+0)$ found in the absence of fluctuations and we obtain the boundary width $u_{\rm smear} \sim \Gamma_l(c\Lambda^2)^2/\Lambda^d|\Delta^{*\prime}(0+)|$. The curvature $\Delta_l''(0) \sim -[\Lambda^d/(c\Lambda^2)^2]|\Delta^{*\prime}(0+)|^2/\Gamma_l$ then diverges as the fluctuations renormalize to zero on large scales.

Physically, $u_{\rm smear}(l)$ can be understood in terms of the *equilibrium* response of a segment of size $L = \Lambda^{-1}e^l$ to the motion of its neighboring regions. Usually, a small displacement of neighboring regions will cause only a small readjustment of the segment of interest within its local energy minimum. The exceptions to this occur when the minimum energy configuration of the segment jumps from one configuration to another as its neighboring regions are slightly displaced: it is these jumps that give rise to the cusp in $\Delta(u)$ in the absence of fluctuations. At non-zero temperature or in the presence of quantum fluctuations, the behavior will not change much except near these jumps, where there will be a range of positions of the neighboring regions over which the segment of concern will have a non-negligible probability to be in *either* of two distinct configurations. This will result in a smearing of the cusp

in $\Delta_l(u)$ over the scale $u_{\rm smear}(l)$ of neighboring region displacements on which this split probability typically occurs. On large scales, the fact that the energy scale grows as L^θ means that it is much less likely that the position of a segment will fluctuate between two energy minima. This is reflected in the renormalization towards zero of Γ_l and the concomitant flow towards zero of the smearing scale $u_{\rm smear} \propto \Gamma_l$. Summarizing, the function $\Delta_l(u)$, whose renormalization is given through equation (28), develops under the RG in the following way: At the scale L_c, $\Delta_l(u)$ is close to its fluctuationless fixed-point function $\Delta^*(u)$, with fluctuations affecting its behavior only in the vicinity of the point $u = 0$ via a smearing of the discontinuity in Δ_l' in a boundary layer whose size is controlled by Γ_l. Once we know how the function $\Delta_l(u)$ evolves, we can substitute it into the other RG equations and see how other quantities renormalize under the RG flow.

In addition to $u_{\rm smear}$, there are two other important displacement scales: the characteristic scale ξ^* of the fixed-point correlator $\Delta^*(u)$ and the scale $u_{\rm vel}$ associated with the velocity $u_{\rm vel} \sim \eta_l v_l / c\Lambda^2$. The latter is the product of the velocity v_l and the characteristic timescale $\eta_l/c\Lambda^2$ of the low-frequency part of the response function $R_l^>(\Lambda, t)$ at wavelengths of the order of the cutoff Λ^{-1}. At scales somewhat larger than the Larkin length $L_c \propto \Lambda^{-1} e^{l_c}$,

$$u_{\rm vel} \ll u_{\rm smear} \ll \xi^*. \tag{42}$$

This is a consequence of the fact that v_l is *exponentially* small ($\propto \exp\{-[S(f)/\hbar]^\alpha\}$) in $\hbar$, while $u_{\rm smear}$ proportional to a *power* of $\hbar_l$ and ξ^* is a static quantity that does not depend on $\hbar_l$ (in the classical case the relevant displacement scales obey the same relation with the role of $\hbar$ played by the temperature T). During the RG flow, $u_{\rm smear}$ decreases gradually with decreasing $\hbar_l$ whereas $u_{\rm vel}$ increases rapidly due to the sharp increase in the viscosity η_l.

Eventually at some scale both $u_{\rm smear}$ and $u_{\rm vel}$ are of the same order. At this scale, which is the crossover scale L_f appearing in the scaling arguments for creep, the functions $\Delta_l'(vt)$ and $\Delta_l''(vt)$ are roughly given by $\Delta^{*\prime}(+0)$ and $\Delta^{*\prime\prime}(+0)$ on the time scales that dominate in Eqs. (29), (31), and (32). At even longer scales, $u_{\rm vel}$ eventually becomes comparable to ξ^*, see Ref. 12. Beyond this scale the randomness is effectively smoothed by the motion of the manifold and can be neglected or treated perturbatively.

In analyzing the renormalization of other quantities by the random pinning forces, we thus see that there are two important regimes:

$$i) \quad u_{\rm vel} < u_{\rm smear}, \quad \text{the nucleation regime,} \tag{43}$$

where we can approximate $\Delta_l'(vt)$ by $\Delta_l'(0) = 0$ and $\Delta_l''(vt)$ by $\Delta_l''(0)$. And

$$ii) \quad u_{\rm smear} < u_{\rm vel} < \xi^*, \quad \text{the depinning regime;} \tag{44}$$

it was argued[12] that this latter regime resembles that of the critical depinning transition[34] in the absence of fluctuations; we can then approximate $\Delta_l'(vt)$ by $\Delta_l^{*\prime}(+0)$ and $\Delta_l''(vt)$ by $\Delta_l^{*\prime\prime}(+0)$. These two regimes are separated by the scale L_f discussed in section III. We will now show how the scale $L_f \sim L_c (f_c/f)^{1/(2-\zeta)}$ naturally appears in the solution of the RG equations and separates the two regimes.

In order to do so we concentrate on the force equation (29) which involves the slope $\Delta_l'(v_l t)$ of the disorder correlator near the origin. The latter is small and vanishes at $u = 0$ for $l < l_c$, hence $\tilde{f}_l = e^{(2-\zeta)l} \tilde{f}$ grows exponentially (since the velocity v_l of the manifold is exponentially small we can neglect the term $\eta_l v_l$ in the equation for $\tilde{f}_l$). In the absence of fluctuations the slope $\Delta_l'(v_l t) \sim \Delta^{*\prime}(0+)$ rapidly turns on as the correlator forms a cusp at l_c; if the disorder term $(\Lambda^d/c\Lambda^2)|\Delta^{*\prime}(0+)|$ overcompensates the scaling term $(2-\zeta)e^{(2-\zeta)l_c}\tilde{f}$, the force will start renormalizing to zero while in the opposite case it will continue to increase. Balancing the two terms we find the critical force density $f_c \sim c\xi/L_c^2$.

Fluctuations smearing the correlator on the scale $u_{\rm smear}$ soften and delay the depinning transition until the growing width $u_{\rm vel}$ of the response function encloses the emerging cusp in $\Delta_l(u)$ at l_f, $u_{\rm vel}(l_f) \sim u_{\rm smear}(l_f)$. Below l_f we have $\Delta_l'(v_l t) \approx \Delta_l'(0) = 0$ and the force increases exponentially $\tilde{f}_l = e^{(2-\zeta)l}\tilde{f}$; starting with a small force $f \ll f_c$, depinning occurs as the cusp emerges at $u_{\rm smear}(l_f) \sim u_{\rm vel}(l_f)$. Replacing again $\Delta_l'(v_l t) \approx \Delta^{*\prime}(0+)$ in (29) we obtain the depinning condition $\tilde{f}_{l_f} \sim (\Lambda^d/c\Lambda^2)|\Delta^{*\prime}(0+)| \sim f_c e^{(2-\zeta)l_c}$; the depinning scale l_f then relates to the force f via $(2-\zeta)(l_f - l_c) \sim \ln(f_c/f)$ or

$$L_f \sim L_c (f_c/f)^{1/(2-\zeta)}. \tag{45}$$

We thus see that the characteristic length scale for creep — the size L_f of the segments that can jump to lower the energy — appears naturally within the RG framework. We emphasize, however, that L_f is entirely determined by *static* properties; so far we have not had to address the crucial issue of dynamic renormalizations — to these we now turn.

The crucial quantity needed for the dynamic renormalization is $\Delta_l''(0)$, which can be obtained from Eq. (28) by comparing $\Gamma_l \Delta_l''(u)$ with the nonlinear terms evaluated at the origin $u = 0$. This yields[12]

$$-\Delta_l{}''(0) \approx \frac{1}{\Gamma_l}\frac{\Lambda^d}{\left(c\Lambda^2\right)^2}\Delta_l'(+0)^2 \tag{46}$$

(see appendix B) and enables us to find the renormalization of the viscosity η_l. Since we are primarily interested in calculating the velocity to exponential accuracy, the calculations simplify significantly. If we do *not* renormalize time scales explicitly, i.e., choosing $z(l) = 0$, the velocity v is given approximately by the viscosity at the scale L_f,

$$\ln v \approx \ln \frac{1}{\eta_{l_f}}. \tag{47}$$

The validity of this condition to exponential accuracy is due to the following argument: At the scale $L_{\rm dyn}$ where $u_{\rm vel} \sim \eta_l v_l/c\Lambda^2 \sim \xi^*$ we have a velocity $v_l \propto 1/\eta_l$ as the effects of pinning are negligible beyond this scale. On intermediate scales, i.e., between L_f and $L_{\rm dyn}$ both η_l and v_l renormalize but *not* exponentially; the only exponentially large renormalization originates from scales between L_c and L_f. Thus, to exponential accuracy, we can ignore the renormalization on scales larger than L_f (and smaller than L_c) and justify (47) (note that, in general, only such dynamic quantities as η_l and v_l are exponentially renormalized, i.e., proportional to $\exp[\pm{\rm const.}L_f^{\tilde\alpha}]$, with $\tilde\alpha$ a positive constant).[39]

The crucial equations for calculating the renormalized velocity are Eqs. (31) and (32). Substituting v_l by zero in these equations and performing the Fourier transformation in Eq. (31) we obtain the two equations

$$\partial_l \kappa_l(\omega) = (4 - d - 2\zeta - z)\,\kappa_l(\omega) - z\omega\partial_\omega\kappa_l(\omega) - \frac{A_d\Lambda^d}{(2\pi)^d}\Delta_l''(0)\frac{\kappa(\omega)}{\left|c\Lambda^2 + D_l(\omega)\right|^2}, \tag{48}$$

$$\partial_l D_l(\omega) = 2D_l(\omega) - z\omega\partial_\omega D_l(\omega) - \frac{A_d\Lambda^d}{(2\pi)^d}\Delta_l''(0)\frac{D_l(\omega)}{c\Lambda^2[c\Lambda^2 + D_l(\omega)]}. \tag{49}$$

Note that Eqs. (48) and (49) are very similar except for the trivial scaling parts. This is the consequence of the quantum fluctuation–dissipation theorem[40] (FDT),

$$\kappa_l(\omega) = \frac{\hbar_l {\rm Im}\left[R_l^>(\Lambda,\omega)\right]}{\left|R_l^>(\Lambda,\omega)\right|^2}\coth\frac{\hbar_l\omega}{2T_l}, \tag{50}$$

which is valid in the quasi-equilibrium situation produced by the long time scales associated with the creep motion. If the relation (50) is satisfied in the bare system ($l = 0$), then Eqs. (48) and (49) guarantee its validity for any l. Strictly speaking the FDT is not applicable for $v \neq 0$, but its appearance here is understood to be consistent with our assumption of being close to local equilibrium and our use of the approximation $v = 0$ in the RG equations for $L < L_f$. Using Eqs. (25), (36), and (50) one can see that the expressions (48) and (49) are identical up to scaling terms.

Substituting Eq. (46) into (49) we obtain

$$\partial_l D_l(\omega) = 2D_l(\omega) - z\omega\partial_\omega D_l(\omega) + \frac{A_d\Lambda^d}{(2\pi)^d}\frac{\Lambda^d}{\left(c\Lambda^2\right)^3}\frac{\Delta_l{}'(+0)^2}{\Gamma_l}\frac{D_l(\omega)}{[c\Lambda^2 + D_l(\omega)]}. \tag{51}$$

Note that Γ_l and $R_l^>(\Lambda, t = 0)$ are functions of l via their dependence on $D_l(\omega)$. Using Eqs. (24), (25), and (50) we can write Γ_l in the form

$$\Gamma_l = -\frac{A_d\Lambda^d}{(2\pi)^d}\int_{-\infty}^{+\infty}\frac{d\omega}{2\pi}\frac{\hbar_l{\rm Im}\left[D_l(\omega)\right]\coth(\hbar_l\omega/2T_l)}{\left|c\Lambda^2 + D_l(\omega)\right|^2}. \tag{52}$$

In a nearly static system $\hbar_l$ and temperature T_l renormalize to zero in a trivial way, see Eqs. (33) and (34), and the elasticity c is not renormalized at all, $\partial_l c = 0$. This is a consequence of the statistical tilt symmetry ($u \to u + \mathbf{b}\cdot\mathbf{z}$, with $\mathbf{b}$ an arbitrary constant vector) of the action (7).

We now concentrate on the zero temperature limit where the correlation function $\Gamma_l = C_l^>(\Lambda, t = 0)$ can be written in the form (cf., (25) and (50))

$$\Gamma_l = \frac{A_d \Lambda^d}{(2\pi)^d} \int_0^\infty \frac{d\omega}{2\pi} \frac{2\hbar_l}{c\Lambda^2 + D_l(i\omega)}. \tag{53}$$

This is a consequence of the identity[40]

$$\int_0^\infty d\omega \, R_l^>(\Lambda, i\omega) = \int_0^\infty d\omega \, \mathrm{Im}[R_l^>(\Lambda, \omega)] \tag{54}$$

following from the analytic structure of the correlator R_l as implied by causality. It is convenient to work within the imaginary time formalism and substitute $\omega \to i\omega$. This substitution transforms the dynamic spectrum into $D_l(i\omega) = \eta\omega + \sum_{k\geq 2} \eta^{(k)} \omega^k$ with the advantage that $D_l(i\omega)$ is real and nonnegative for positive ω. The calculation of the velocity v of the driven elastic manifold reduces to the problem of solving the equation

$$\begin{aligned} \partial_l D_l(i\omega) &= 2D_l(i\omega) - z\omega \partial_\omega D_l(i\omega) \\ &+ \frac{A_d \Lambda^d}{(2\pi)^d} \frac{\Lambda^d}{(c\Lambda^2)^3} \frac{{\Delta_l}'(+0)^2}{\Gamma_l} \frac{D_l(i\omega)}{[c\Lambda^2 + D_l(i\omega)]}, \end{aligned} \tag{55}$$

with the initial condition $D_0(i\omega) = \eta|\omega| + \rho\omega^2$ (valid for any ω) and calculating the renormalized low-frequency viscosity $\eta_l = \partial_\omega D_l(i\omega)$, $\omega \to 0$; having found η_l we can determine the velocity v using the relation (47). Note that if $D_0(i\omega) = D_0(-i\omega)$ then this property is preserved under the RG transformation.

On very short scales $l < l_c$ the disorder-dependent term on the right-hand side of (55) can be neglected. On intermediate scales $l_c < l < l_f$ we can substitute ${\Delta_l}'(+0)$ by its fixed-point value which is related to the bare potential through (see appendix B)

$${\Delta^*}'(+0)^2 \simeq \epsilon e^{(\epsilon - 2\zeta) l_c} \frac{(c\Lambda^2)^2}{\Lambda^d} \Delta(0) \sim \frac{(c\Lambda^2)^4}{\Lambda^{2d}} \xi^2 e^{-2\zeta l_c}, \tag{56}$$

where we have used the relation $\Delta(0) \sim c^2 \xi^2 (\Lambda / e^{l_c})^\epsilon$ in the last equation.

C. Naive RG and "Localization" Transition

Before embarking on the complete analysis it is instructive to see what happens if we simply keep the leading low-frequency form of $D(i\omega)$ as is conventionally done in dynamic renormalization group calculations. To do this we substitute the Ansatz $D_l(i\omega) = \eta_l|\omega|$ for *all* frequencies into (53). Calculating the integral we easily obtain $\Gamma_l \sim \left(\hbar_l \Lambda^d / \eta_l\right) \ln\left(\eta_l \bar{\omega} / c\Lambda^2\right)$, where we have introduced a high-frequency cutoff $\bar{\omega}$. Substituting this expression into (55) and approximating

$$D_l(i\omega) / \left(c\Lambda^2 + D_l(i\omega)\right) \to D_l(i\omega) / c\Lambda^2 = \eta_l \omega / c\Lambda^2, \tag{57}$$

i.e., assuming that the low-frequency asymptotics $D_l(i\omega) = \eta_l \omega$ is valid for any ω and l, we obtain the equation for the renormalized friction coefficient

$$\partial_l \eta_l \sim \frac{S_\eta}{\hbar \eta} e^{-(d+2\zeta) l_c} \, \eta_l^2, \tag{58}$$

with $S_\eta \sim \eta \xi^2 L_c^d$. Unfortunately, the behavior of this equation is pathological: one can see that it would imply a divergence of η_l at a *finite* length scale. This would presumably mean that the velocity goes to zero in the presence of a nonzero force and quantum fluctuations, a result that appears to be implausible. Of course, what one must check in any situation where some parameter in an effective action diverges under the RG flow is, whether this is due to an unphysical restriction of the space of relevant parameters, a breakdown in whatever approximations that have been made in deriving the RG flow, or some other effect. In our case, it will turn out that the renormalization of the whole frequency spectrum is very important. This should be contrasted with the classical case for which one can obtain the result $v \propto \exp[-U(f)/T]$ by considering the low-frequency limit only[12].

D. RG Analysis of Dynamic Response

We now turn to the analysis of the RG flow equations (55) and (56). In order to find the flow of the function $D_l(\omega)$ it is convenient to make the unconventional choice $z(l) = 0$ and allow η_l to change arbitrarily. If one is more comfortable with a flowing dynamical exponent $z(l)$, one can work more generally with the quantity

$$E_l(\Omega) = D_l(i\Omega)/c\Lambda^2, \tag{59}$$

where $\Omega \equiv \omega \exp[-\int^l dl' z(l')]$ represents the unrenormalized frequency; substituting (59) into (55) and accounting for (56) as well as the trivial renormalization of $\hbar_l$, see (34), we arrive at

$$\begin{aligned}\partial_l E_l(\Omega) &\approx 2E_l(\Omega) + Ke^{(d+2\zeta-2)l}\frac{E_l(\Omega)\Theta(l-l_c)}{1+E_l(\Omega)}\frac{1}{\int_{-\infty}^{+\infty}\frac{\eta d\Omega/c\Lambda^2}{1+E_l(\Omega)}} \\ &\equiv 2E_l(\Omega) + \frac{E_l(\Omega)\Theta(l-l_c)}{1+E_l(\Omega)}B_l,\end{aligned} \tag{60}$$

with the dimensionless constant K given by

$$K = 2\pi\epsilon\frac{\eta\Delta(0)}{(c\Lambda^2)^2\hbar}e^{-(d+2\zeta-4)l_c} \sim \frac{S_\eta}{\hbar}e^{-(d+2\zeta)l_c} \tag{61}$$

and

$$B_l = \frac{Ke^{(d+2\zeta-2)l}}{\int_{-\infty}^{+\infty}\frac{\eta d\Omega/c\Lambda^2}{1+E_l(\Omega)}} \sim \frac{U(L)}{\int_{-\infty}^{+\infty}\frac{\hbar d\Omega}{1+E_l(\Omega)}}. \tag{62}$$

For $l < l_c$ the renormalization of the dynamics due to disorder can be neglected, as properly expressed by the step function $\Theta(l - l_c)$ in (60). The quantity $B_l \propto 1/\Gamma_l$ governs the fluctuation-induced smearing of the cusp in the force-force correlator. The right-hand side of (60) behaves differently for $E_l(\Omega) \ll 1$ and $E_l(\Omega) \gg 1$; using the approximation

$$\frac{E_l(\Omega)}{1+E_l(\Omega)} \approx \min\left(E_l(\Omega), 1\right) \tag{63}$$

considerably simplifies the analysis but does not change the result qualitatively. We rewrite (60) in the corresponding (l-dependent) frequency regions in the form

$$\partial_l E_l(\Omega) \approx 2E_l(\Omega) + E_l(\Omega)B_l, \quad E_l(\Omega) < 1, \tag{64}$$

$$\partial_l E_l(\Omega) \approx 2E_l(\Omega) + B_l, \quad E_l(\Omega) > 1. \tag{65}$$

As is readily seen from (64) and (65) the function $E_l(\Omega)$ is an increasing function of l for all Ω and $E_l(\Omega) \to \infty$ as $l \to \infty$. In addition, if $E_0(\Omega)$ is a monotonically increasing function of Ω then $E_l(\Omega)$ remains monotonic in Ω for any l. Let us define the frequency $\tilde{\Omega}_l$ and the scale $\tilde{l}_\Omega$ which solve the equation

$$E_l(\Omega) = 1; \tag{66}$$

the function $\tilde{\Omega}_l$ starts at $l = 0$ with a finite value $\tilde{\Omega}_0$ and decreases with increasing l. For any $l > 0$ we distinguish between the three regions $0 < \Omega < \tilde{\Omega}_l$, $\tilde{\Omega}_l < \Omega < \tilde{\Omega}_0$, and $\tilde{\Omega}_0 < \Omega$, see Fig. 3.

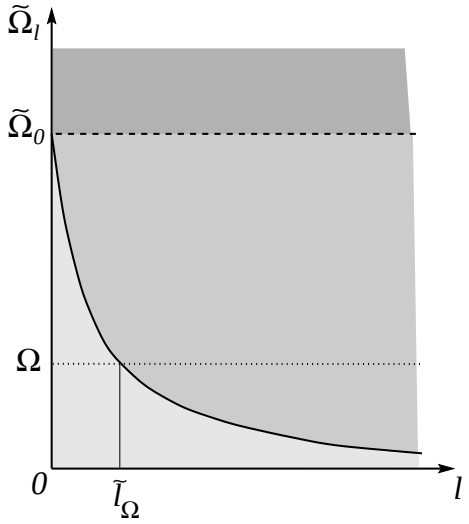

FIG. 3. Different regimes relevant in the integration of the dynamical equation (60): For $\Omega < \tilde{\Omega}_0$ the integration is split into two regimes $0 < l < \tilde{l}_\Omega$ and $\tilde{l}_\Omega < l$, while for $\Omega > \tilde{\Omega}_0$ the integration involves only one regime.

In each of these regions the function $E_l(\Omega)$ can be found explicitly in terms of $E_0(\Omega)$ and the yet-to-be-determined function B_l,

$$E_l(\Omega) = E_0(\Omega) \exp\left[2l + \int_0^l dl' B_{l'}\right], \quad 0 < \Omega < \tilde{\Omega}_l, \tag{67}$$

$$E_l(\Omega) = e^{2(l-\tilde{l}(\Omega))}\left[1 + \int_{\tilde{l}(\Omega)}^l dl' e^{-2\left(l'-\tilde{l}(\Omega)\right)} B_{l'}\right], \quad \tilde{\Omega}_l < \Omega < \tilde{\Omega}_0, \tag{68}$$

$$E_l(\Omega) = E_0(\Omega)e^{2l} + e^{2l}\int_0^l dl' e^{-2l'} B_{l'}, \quad \tilde{\Omega}_0 < \Omega. \tag{69}$$

Note that we integrate (64) and (65) subsequently in the first two regions $0 < l < \tilde{l}_\Omega$ and $\tilde{l}_\Omega < l$, while for $\Omega > \tilde{\Omega}_0$ equation (65) applies for all values of l. Correspondingly, the integral $\int_{-\infty}^{+\infty} d\Omega/[1 + E_l(\Omega)]$ that determines B_l, see (62), can be written as a sum of three terms. We will show below that B_l increases exponentially, implying that the boundary $\tilde{\Omega}_l$ is exponentially small and the first integral extending over the interval $0 < \Omega < \tilde{\Omega}_l$ can be neglected, hence

$$\frac{1}{2}\int_{-\infty}^{+\infty} d\Omega \frac{1}{1+E_l(\Omega)} \approx \int_{\tilde{\Omega}_l}^{\tilde{\Omega}_0} \frac{d\Omega}{1 + e^{2(l-\tilde{l}(\Omega))}\left[1 + \int_{\tilde{l}(\Omega)}^l dl' e^{-2\left(l'-\tilde{l}(\Omega)\right)} B_{l'}\right]} + \int_{\tilde{\Omega}_0}^{+\infty} \frac{d\Omega}{1 + E_0(\Omega)e^{2l} + e^{2l}\int_0^l dl' e^{-2l'} B_{l'}} \tag{70}$$

$$\approx \int_0^{\tilde{\Omega}_0} \frac{d\Omega}{1+G_l} + \int_{\tilde{\Omega}_0}^{\infty} \frac{d\Omega}{1 + E_0(\Omega)e^{2l} + G_l}. \tag{71}$$

In the last equation we have approximated $\tilde{\Omega}_l \approx 0$ and $\tilde{l}(\Omega) \approx 0$ and have introduced the expression

$$G_l \equiv e^{2l}\int_0^l dl' B_{l'} e^{-2l'} \approx \frac{B_l}{d\ln B_l/dl - 2}; \tag{72}$$

the last approximation applies if B_l increases faster than e^{2l}. Substituting $E_0(\Omega) = \left(\eta\Omega + \rho\Omega^2\right)/c\Lambda^2$ (see (38) and (59)) into (71) we see that the second integral on the right-hand side of (71) always dominates and we conclude that it is the *high-frequency* behavior of $D_0(\omega)$ that controls the large length scale renormalization of the dynamics.

Using the definition of B_l, see (62) and evaluating the integrals over Ω explicitly we obtain an implicit equation for B_l valid at large length scales

$$B_l \sim \frac{K e^{(d+2\zeta-2)l}}{\min\left[e^{-2l}\ln\frac{e^{2l}\eta^2/\rho}{G_l c\Lambda^2}, e^{-l}\frac{\eta/\sqrt{\rho}}{\sqrt{G_l c\Lambda^2}}\right]}, \tag{73}$$

where we have ignored multiplicative factors of order unity. The first term in the denominator applies for small ρ at intermediate length scales when G_l is not too large, while the second is relevant if the inertia is substantial ($\rho > \eta^2 e^{2l}/c\Lambda^2 G_l$) and for asymptotically large scales for *any* non-zero ρ. Given that the approximation in (72) is valid, as is the case in the regimes of interest, we have a non-linear differential equation for B_l; in its simplest approximation with $G_l \approx B_l$ this reduces to an algebraic equation which is readily solved. Using the definition of K, Eq. (61) and the expressions $L_c = \Lambda^{-1}e^{l_c}$, $U_c \sim c(\xi^2/L_c^2)L_c^d$, $S_\eta \sim \eta\xi^2 L_c^d$, and $S_\rho^2 \sim \rho\xi^2 U_c L_c^d$, we find the result

$$B_l \sim \frac{\rho}{\eta}\frac{c\Lambda^2}{\eta}K^2\left[e^{(d+2\zeta-1)l}\right]^2 \sim \left[\frac{S_\rho}{\hbar}e^{(d+2\zeta-1)(l-l_c)}\right]^2 \tag{74}$$

in the *inertial case*. The behavior is rather more complicated for the dissipative case: at intermediate length scales we have

$$B_l \sim \frac{K\, e^{(d+2\zeta)l}}{\ln[(\eta^2/\rho c\Lambda^2 K)e^{-(d+2\zeta-2)l}]} \sim \frac{S_\eta}{\hbar}\frac{e^{(d+2\zeta)(l-l_c)}}{\ln[(S_\eta\hbar/S_\rho^2)e^{-(d+2\zeta-2)(l-l_c)}]} \tag{75}$$

which increases slightly *faster* with length scale than in the absence of the logarithmic factor. The crossover between the dissipative and massive results appears at

$$B_{l_I} \sim K\frac{\eta^2}{\rho c\Lambda^2}e^{2l_I} \sim \frac{S_\eta^2}{S_\rho^2}e^{2(l_I-l_c)}; \tag{76}$$

comparing with (75) this translates into the length scale

$$L_I \sim L_c\left(\frac{S_\eta\hbar}{S_\rho^2}\right)^{1/(d-2+2\zeta)}, \tag{77}$$

with a corresponding energy scale

$$U_I \sim U_c\left(\frac{L_I}{L_c}\right)^{(d+2\zeta-2)} \sim U_c\frac{S_\eta\hbar}{S_\rho^2} \sim \frac{\hbar\eta}{\rho}. \tag{78}$$

For $L > L_I$ the behavior of B_l is always dominated by the inertia and the result (74) takes over.

In the end we see that the coefficient $B_l \propto 1/\Gamma_l$ describing the fluctuations rounding the cusp in the correlator Δ_l increases dramatically with increasing scale l (with a correspondingly decreasing Γ_l). Substituting $E_l \to E_0 e^{2l} + G_l \to B_l + (\Omega/\Omega_c)^\alpha$ in the integral of (62), we see that the integration is squeezed to the high energy side where it is ultimately cutoff by the inertial term ($\alpha = 2$) or a more general cutoff $(\Omega/\Omega_c)^\alpha$. Hence the remaining high-frequency fluctuations measured with respect to the typical barriers $U(L)$ at this scale determine the smoothing coefficient Γ_l. Technically, the exponent in the non-Arrhenius type law (74) then appears via solution of the implicit equation for B_l with the result $B_l \propto 1/\hbar^\alpha$. For the extreme case with a linear spectrum sharply cut at the frequency Ω_c, $D_0(i\omega < i\omega_c) = \eta\omega$ and $D_0(i\omega > i\omega_c) = \infty$, a similar calculation provides an action that is *exponentially* (rather than power-law) enhanced in the limit of small forces f.

Substituting the expressions for B_l into the equation for E_l we can find how the dynamic spectrum $D_l(i\omega)$ is renormalized. At low frequencies

$$\partial_l D_l(i\omega \to i0) \sim [2 + B(l)]D_l(i\omega \to i0), \tag{79}$$

and hence $D_l(i\omega \to 0) \propto \exp\left[2l + \int_0^l dl' B_{l'}\right]$; consequently the renormalized viscosity η_f on the scale l_f is

$$\eta_{l_f} \approx \eta \exp\left[2l_f + \int_0^{l_f} dl' B_{l'}\right] \tag{80}$$

(note that if we had used the conventional normalization in the action, adjusting the dynamic exponent $z(l)$ to keep η_l fixed, we would have obtained the same results for physical quantities but the renormalization would have gone into $z(l) = 2 + B_l$ rather than the friction coefficient η_l).

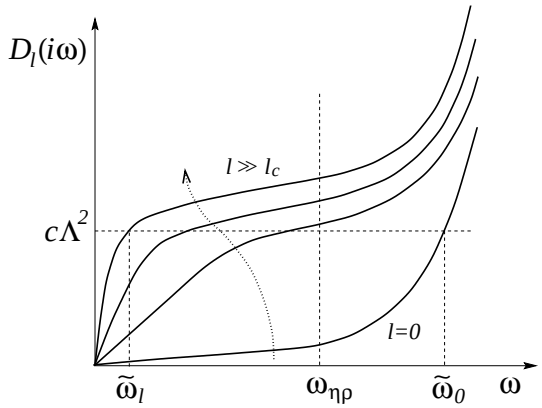

FIG. 4. Schematic renormalization of the dynamic spectrum $D_l(i\omega)$ for a dissipative/massive initial dynamics, $D_0(i\omega) = \eta|\omega| + \rho\omega^2$, with a crossover at $\omega_{\eta\rho} = \eta/\rho$. The spectrum is renormalized differently on small and large frequencies: in the region $D_l(i\omega) \ll c\Lambda^2$ the spectrum is double–exponentially enhanced and grows as $\eta|\omega| \exp[\text{const.}e^{\beta l}]$, with $\beta > 0$ an exponent depending on the specific dynamics. For $D_l(i\omega) \gg c\Lambda^2$ the renormalization takes the different form $D_l(i\omega) \approx \eta\omega e^{(2-z)l} + \rho\omega^2 e^{(2-2z)l} + F_l$, with F_l independent of the frequency ω.

Going back to the dynamical equation (60), we see that B_l not only determines the low-frequency part but the entire function $D_l(i\omega)$ (we assume $z = 0$ and identify Ω with ω). A schematic renormalization of the dynamic spectrum $D_l(i\omega)$ is shown in Fig. 4: the low-frequency part at $\omega < \tilde{\omega}_l \sim (c\Lambda^2/\eta)\exp(-B_l)$ where $D_l < c\Lambda^2$ remains linear, $D_l(i\omega) \sim \eta_l\omega$, but is boosted exponentially with $\eta_l \sim \eta\exp(B_l)$ (with B_l itself growing exponentially in l). At frequencies above $\tilde{\omega}_l$ the upward renormalization is reduced and the response $D_l(i\omega)$ develops a flat intermediate regime. Finally, at high frequencies $\omega > \tilde{\omega}_0$ the renormalization remains small, while the shape of the dynamical response again reflects the form of the original bare dynamics D_0 with an additional shift $\propto c\Lambda^2 B_l$. It is this high-frequency part of D_l that dominates the important renormalization of η_l at low frequencies. We attribute the strongly renormalized low-frequency part $D_l < c\Lambda^2$ to those degrees of freedom of the manifold describing its inter-valley motion, while the remaining modes at intermediate and high frequencies describe its intra-valley motion smoothing the disorder landscape. In the next section we will discuss the meaning, significance, and problematic aspects of the unusual dynamical renormalization scheme uncovered above.

E. Results: Quantum Creep

The physical quantities of primary interest can be obtained from the analysis of the previous section. In particular, using the relation (47) we find the creep velocity at low forces in the inertial case,

$$v \propto \exp\left\{-\left[\frac{S_\rho}{\hbar}\left(\frac{f_c}{f}\right)^{(d+2\zeta-1)/(2-\zeta)}\right]^2\right\}, \tag{81}$$

with an unknown multiplicative coefficient of order unity incorporated into S_ρ. In the dissipative case there is a characteristic crossover force

$$f_I \sim f_c\left(\frac{\rho U_c}{\hbar\eta}\right)^{2/(d-2+2\zeta)} \tag{82}$$

that separates two distinct regimes: For intermediate forces $f_I \ll f \ll f_c$ we have

$$v \propto \exp\left[-\frac{S_\eta}{\hbar}\left(\frac{f_c}{f}\right)^{(d+2\zeta)/(2-\zeta)}\frac{1}{\ln(f/f_I)}\right] \tag{83}$$

with an unknown constant coefficient incorporated into S_η. But at asymptotically low forces $f \ll f_I$ the inertial term in the action dominates and the behavior of the velocity crosses over to the inertial result (81). For the dissipative

case, the result is similar to that obtained using scaling arguments in section III B in the *intermediate* regime, but the logarithmic factor causes the velocity to decrease slightly faster with decreasing force than anticipated. By contrast, in the inertial case the creep velocity is much smaller that anticipated: it can be written in the form $v \propto \exp\left[-(S_{\rm mass}(f)/\hbar)^2\right]$, with $S_{\rm mass}(f)$ the characteristic action obtained in section III C using scaling arguments. At asymptotically low forces, this result is also valid for the more general model including a dissipative dynamics at low frequencies and an inertial dynamics at high frequencies.

F. Results: Classical Creep and Crossover

At high temperatures the coefficient $\Gamma_l = C_l^>(\Lambda, t=0)$ is independent of the dynamics and the evolution of the spectrum $D_l(i\omega)$ does not feed back into Γ_l. Equation (79), written in terms of the bare temperature, then takes the form

$$\partial_l D_l(i\omega \to 0) \sim \frac{U(L)}{T} D_l(i\omega \to 0). \tag{84}$$

Using the relations (47), $U(L) \sim U_c(L/L_c)^{(d+2\zeta-2)}$, $L \sim L_c(f/f_c)^{1/(2-\zeta)}$, we obtain the classical creep law $v(F) \sim \exp[-U(f)/T]$ with $U(f) \sim U_c(f_c/f)^{(d+2\zeta-2)/(2-\zeta)}$, see Ref. 12. The exponent $\theta = d + 2\zeta - 2$ that determines the scaling of $U(L)$ is simply the scaling dimensionality of the temperature, see (33), in terms of which (84) can be written with a prefactor $U(L)/T \sim U_c/T_l \sim e^{(d+2\zeta-2)(l-l_c)}U_c/T$.

One can find the crossover temperature from classical to quantum creep by comparing the exponents in (83) and (81) with $U(f)/T$. For the inertial case,

$$T_{\rm cr} \propto f^{(d+2\zeta)/(2-\zeta)}, \tag{85}$$

which is different from the naive result obtained via simple scaling arguments, see section III. For the dissipative case, the crossover temperature depends on the regime. For intermediate forces, it is the same as that given by the naive scaling arguments (up to a logarithmic factor), but for $f \ll f_I$ the crossover temperature is again given by the result (85) for the inertial case.

G. Interpretation

As mentioned earlier, a dependence on $\hbar$ of the form (81) might be expected if the dynamics were dominated by atypical barriers. A simple example is given by a classical particle diffusing in a short-range correlated random potential. At positive temperatures there is a linear response to an external force with the inverse mobility of the particle proportional to $\int dU \mathcal{P}(U) \exp(U/T)$, where $\mathcal{P}(U)dU$ is the probability density of barriers U. For the case of a Gaussian distribution of the random potential, we see that $v \propto f \exp(-\text{const.}/T^2)$, resulting in a non-Arrhenius temperature dependence.

Analogous effects can occur in quantum transport: Consider a quantum particle of mass m and with a dissipative coefficient η_l, tunneling through a succession of barriers of random heights U but, for simplicity, uniform width a. The inverse mobility of such a particle can be written as

$$\frac{1}{\mu} \propto \int dU \mathcal{P}(U) \exp\left(\frac{\eta a^2}{\hbar} + \frac{\sqrt{mU}a}{\hbar}\right). \tag{86}$$

The exponent contains a sum of two actions, the first due to dissipation and the second describing the inertial response. One can see that even if the dissipation is strong, in the limit $\hbar \to 0$ the inertial effects can dominate: the integral in (86) is calculated using the method of steepest descent and since the massive contribution to the action is proportional to $\sqrt{U}$, it will contribute a term larger than the dissipative one. In particular, with a Gaussian distribution of barriers of the form $\mathcal{P}(U) \sim \exp[-(U/U_0)^2]$ this leads to $\mu \propto \exp[-(\sqrt{mU_0}a/\hbar)^{4/3}]$ and we obtain a similar non-trivial dependence on $\hbar$ as found above in (81) for the creeping elastic manifolds of interest here.

In this simple single-particle example it is easy to understand what is going on: Because the particle must tunnel through a succession of barriers, the dynamics is dominated by the largest ones as long as there is a sufficiently long tail to the barrier distribution; the smaller the quantum fluctuations, the larger the barriers that dominate. For the probability distribution function $\mathcal{P}(U)$ chosen above, $U \simeq \left(\sqrt{m}aU_0^2/\hbar\right)^{2/3} \to \infty$ for $\hbar \to 0$. The form of the tail of the distribution of barriers thus dominates the mobility and gives rise to the unusual dependence on $\hbar$. The fact that

for small $\hbar$ the dominant barriers are high implies that the characteristic time scale for tunneling through the barrier is short (in the above case the time τ is given through $\tau \simeq a\sqrt{m/U}$); this is what causes the long-time behavior as manifested in the mobility to be dominated by the inertia rather than by the dissipative response. In the case of interest here, the elastic manifold, the barriers that must be surmounted depend on the driving force — the lower the force, the higher these barriers are. If one assumes that the barriers relevant for tunneling have an unbounded distribution similar to the toy model studied above, it is not surprising that it is the inertial dynamics that dominates the limit of low forces.

However, the reason for the anomalous dependence on $\hbar$ is more subtle for the elastic manifold with its many degrees of freedom. As can be seen from the analysis in the previous section, the anomalous dependence can be traced back to the dependence of the quantum fluctuations on one length scale, as parametrized by Γ_l, on the random pinning at smaller scales. Very crudely, this might be interpreted as leading to an increase of the *effective mass density* with length scale caused by the motion of smaller scale sections of the manifold implicit in the tunneling motion of a segment of size L_f. Determining whether or not this is a reasonable interpretation must wait for a better understanding of the physics underlying the RG results and whether these are valid.

V. VALIDITY OF RG RESULTS

In both the previous and the present work on classical and quantum creep of elastic manifolds the validity of the approximations that underly the RG formulation have not been carefully examined. In unpublished work[41] one of the problematic aspects, the possible effects of tails in the distribution of local effective friction coefficients, has been investigated. Here, we briefly summarize the potential problems that this suggests as well as more basic ones that have not, to our knowledge, been raised previously.

A. Random Friction

One difficulty, analyzed in Ref. 41, is already apparent in the toy model of a single particle in a random potential: the broad distribution of times to go through or over barriers. In particular, as discussed in section IV E above, for a single particle the mobility is dominated not by the typical or even the average rate for overcoming the local barriers, but by the *average time* to overcome them; and the average time is dominated by anomalously large barriers. As this problem already arises in the classical case both in the toy model and for elastic manifolds, we restrict our discussion to the simpler classical limit.

The main idea of the RG is to derive equations which relate the renormalized parameters of the field theory to the bare ones. Very often the parametric space of the bare and renormalized theories are identical. In other words, if the bare theory is described by the parameter set $\alpha_0^{(1)}, \alpha_0^{(2)} \ldots$ the renormalized theory will be described by the same set of variables $\alpha_l^{(1)}, \alpha_l^{(2)} \ldots$. An example of this kind of RG is the ϕ^4 theory to one-loop order. It could be, however, that under the RG flow additional variables $\beta_l^{(1)}, \beta_l^{(2)} \ldots$ are generated even if their bare values are zero. These variables might be strongly relevant and feed back to the original set of parameters. An example of such a behavior, which we could handle successfully, has already been considered above: in order to obtain sensible results we had to introduce a function $D_l(i\omega)$ describing the dynamics on *all* frequencies. In this paragraph we will show that another set of dangerous variables is generated under the RG flow — these variables describe the probability distribution function of waiting times. In the RG scheme considered above the most crucial quantity is the renormalized viscosity η_l which is proportional to the waiting time at the scale l. We will show that the randomness due to the point-like disorder will produce a random and spatially inhomogeneous distribution of frictions which appears to be very broad and hence cannot be properly described by its first moment η_l alone.

Let us then consider randomness in the local effective friction coefficients from the beginning and assume that the friction η is a function $\eta = \eta[u(\mathbf{z}), \mathbf{z}]$ of both the displacement $u(\mathbf{z})$ and the internal coordinate $\mathbf{z}$ of the manifold. The local η has the natural interpretation as a characteristic time to overcome barriers involving the smaller length scale deformations that have already been integrated out. The simplest case to consider is a random potential that is periodic in u with a locally random phase shift; such a model is applicable to charge density waves (CDWs). Because of the periodicity, for CDWs we can expand the function $\eta(u, \mathbf{z})$ into the Fourier series and there will be a component that is independent of u and only depends on $\mathbf{z}$; we consider the effects of such randomness here.

We assume that $\eta(\mathbf{z})$ is a random short-range correlated variable with cumulants $\eta^{(n)}$; e.g., the first three take the form $\overline{\eta(\mathbf{z})} = \eta^{(1)} \equiv \eta$, $\overline{\eta(\mathbf{z})\eta(\mathbf{z}')} - \overline{\eta(\mathbf{z})}\,\overline{\eta(\mathbf{z}')} = \eta^{(2)}\delta(\mathbf{z} - \mathbf{z}')$, and

$$\overline{\eta(\mathbf{z})\eta(\mathbf{z}')\eta(\mathbf{z}'')} - \overline{\eta(\mathbf{z})\eta(\mathbf{z}')}\ \overline{\eta(\mathbf{z}'')} - \overline{\eta(\mathbf{z}'')\eta(\mathbf{z}')}\ \overline{\eta(\mathbf{z})} - \overline{\eta(\mathbf{z}'')\eta(\mathbf{z})}\ \overline{\eta(\mathbf{z}')} + 2\overline{\eta(\mathbf{z})}^3$$
$$= 2\eta^{(3)}\left[\delta\left(\mathbf{z}-\mathbf{z}'\right)\delta\left(\mathbf{z}-\mathbf{z}''\right) + \delta\left(\mathbf{z}'-\mathbf{z}''\right)\delta\left(\mathbf{z}'-\mathbf{z}\right) + \delta\left(\mathbf{z}''-\mathbf{z}\right)\delta\left(\mathbf{z}''-\mathbf{z}'\right)\right]. \tag{87}$$

Note that we define cumulants $\eta^{(n)}$ up to a factor $n!$. After averaging over the randomness the classical MSR-action (7) will have additional terms of the form

$$A_{\rm rand} = \sum_{n\geq 2} A^{(n)} = \sum_{n\geq 2} (-1)^n \eta^{(n)} \int d^d z dt_1 \dots dt_n\, \dot{u}(\mathbf{z},t_1) iy(\mathbf{z},t_1) \dots \dot{u}(\mathbf{z},t_n) iy(\mathbf{z},t_n). \tag{88}$$

When deriving the RG equations with an action that includes terms of the form $A_{\rm rand}$, it is necessary to find the average over fast modes of terms containing products of two perturbations, in particular, terms of the form

$$\delta A = \frac{1}{2}\left\langle A_{\rm rand} \int d^d z \tau_1 d\tau_2\, \Delta_l\left[u(\mathbf{z},\tau_1) - u(\mathbf{z},\tau_2)\right] iy(\mathbf{z},\tau_1) iy(\mathbf{z},\tau_2)\right\rangle_>, \tag{89}$$

with $\langle \dots \rangle_>$ the standard RG average over fast modes. Making use of (88), the average (89) can be written as a sum of terms involving the cumulants $\eta_l^{(n)}$ (see appendix C for details; here, we summarize the main ideas of the calculation). The term of order n in (89) then generates $2n$ terms proportional to $\delta A_1^{(n)}$,

$$\delta A_1^{(n)} = (-1)^n \eta_l^{(n)} \Delta_l''(0) \int d^d z dt_1 \dots dt_n\, \dot{u}(\mathbf{z},t_1) iy(\mathbf{z},t_1) \dots \dot{u}(\mathbf{z},t_n) iy(\mathbf{z},t_n) \tag{90}$$

which feed back to the term (88). In addition, there are $4n^2 - 4n$ terms proportional to $\delta A_2^{(n)}$,

$$\delta A_2^{(n)} = (-1)^n \eta_l^{(n)} \int d^d z dt_1 \dots dt_n\, \dot{u}(\mathbf{z},t_1) iy(\mathbf{z},t_1) \dots$$
$$\dot{u}(\mathbf{z},t_n) iy(\mathbf{z},t_n) \Delta_l''\left[u(\mathbf{z},t_1) - u(\mathbf{z},t_2)\right]. \tag{91}$$

These renormalizations involve the behavior of the correlator $\Delta_l(u)$ at the origin whose growth at long length scales is crucial for the renormalization group analysis, see the above discussion. We can keep track of the most dangerous terms by substituting $\Delta_l''(u)$ by $\Delta_l''(0)$ in (91). The renormalization of the cumulants $\eta_l^{(n)}$ from the above process can be written in the form

$$\partial_l \eta_l^{(n)} \propto -\Delta_l''(0)\left(2n^2 - n\right)\eta_l^{(n)}; \tag{92}$$

furthermore, there are non-linear terms that create higher moments from lower moments, see appendix C. As $-\Delta_l''(0)$ grows exponentially with l, i.e., as a power of the length scale, the cumulants $\eta_l^{(n)}$ grow very rapidly. The n^2 coefficient and the positivity of $-\Delta_l''(0) \propto 1/T_l \propto e^{\theta l}$ in Eq. (92) imply that the high order moments grow so fast that ratios of the form $\eta_l^{(n)}/\eta_l^n$, which naively are expected to be dimensionsless (in the RG sense), *themselves* grow exponentially with increasing length scale. Indeed, the high order moments increase so rapidly with n that, if these results are taken literally, the distribution of $\eta_l(\mathbf{z})$ has such a long tail that it is not uniquely determined by its moments — and it is certainly not well characterized by its mean $\overline{\eta_l(\mathbf{z})} = \eta_l$. Note that a random friction $\eta_l(\mathbf{z})$ is not dangerous near the zero-temperature depinning transition ($f - f_c \ll f_c$) as in this case $\Delta_l''(0)$ should be substituted by $\Delta_l''(0+) > 0$ and Eq. (92) suggests that $\eta_l^{(n)}$ renormalizes to zero for any n (although it will actually be stabilized at a small value of the order of an n-dependent power of ϵ because of other terms).

The analysis in appendix C shows that even if initially the friction is non-random, the disorder term alone will generate the corrections to the second cumulant. The second cumulant will then generate the third cumulant to the next loop order, and so forth. As the cumulants grow extremely rapidly, the RG flow becomes essentially uncontrollable. However note, that there is still an approximation in the above analysis: we have substituted the argument of the second derivative of the disordered correlator $\Delta_l''(u)$ by zero in Eq. (91). In order to be accurate we have to include the terms of the form

$$\delta A_2^{(n)} = (-1)^n \eta_l^{(n)} \int d^d z dt_1 \dots dt_n\, \dot{u}(\mathbf{z},t_1) iy(\mathbf{z},t_1) \dots$$
$$\dot{u}(\mathbf{z},t_n) iy(\mathbf{z},t_n) \sum_{i\neq j}^{n} F_l\left[u(\mathbf{z},t_i) - u(\mathbf{z},t_j)\right], \tag{93}$$

cf. Eq. (91), into the action, i.e., we have to renormalize one more function $F_l(u)$. Under the RG transformation this function will produce a new set functions, and so forth — it is presently unclear how all these variables can be analyzed in a regular way.

One way that one might hope to make progress is to rewrite the equations of motion so that instead of having to deal with a random η on the left hand side, one works with a random mobility $\mu = 1/\eta$ on the right hand side. This quantity, as it is bounded from above by the fastest motion, is unlikely to have troublesome long tails in its distribution. But the appearance of a random mobility multiplying all the spatially random pinning forces introduces additional technical complications into the formalism and it is presently not clear how to handle them. Nevertheless, there are a lot of constraints on the renormalization, e.g., the *static* response will not be modified by the randomness of either the pinning or the mobility at any wavelength. Whether this is enough to make possible a fully controlled analysis of at least the classical thermal creep regime is an interesting challenge.

B. Underlying Formulation

It is possible that the apparent runaway of the distribution of the local friction coefficients is indicative of a breakdown in the basic scaling assumption that underlies this and earlier work: If the barriers for motion scale with an exponent ψ that is larger than the exponent $\theta = d-2+2\zeta$ controlling the scaling of fluctuations in minimal energies and the renormalization of the inverse temperature, then the present scheme where the dynamics is controlled by static properties, such as the correlator $\Delta(u)$, cannot be valid. One then has to take into account all the dangerous variables discussed above.

It is instructive to go back to the original formulation of the RG expansion for the depinning in the absence of fluctuations[33], henceforth NF. In the derivation of the ϕ^4 theory from the Ising model for conventional equilibrium phase transitions, the starting point is an expansion around a mean field theory and the actual "field" $\phi(\mathbf{x})$ used in the RG formulation is closely related to the local effective field — applied plus exchange — acting on a spin rather than to the spin itself. If the interactions are long but finite range, these fields will be slowly varying in space and weakly fluctuating, enabling a systematic expansion to be started.

NF focus on one segment $\mathbf{z}$ and use the linear combination $u(\mathbf{z},t)$ of the displacements of *other segments* that determine the elastic force on $\mathbf{z}$ as the basic field, which is hence intrinsically a coarse-grained quantity. The underlying local displacements we will here call $w(\mathbf{z},t)$. The segment $\mathbf{z}$ feels a linear restoring force proportional to $u(\mathbf{z},t)-w(\mathbf{z},t)$, plus the applied driving force, plus a quenched random pinning force that is a function of $w(\mathbf{z})$, and thermal noise. The vertices in the effective field theory are given by correlations and responses of $w(\mathbf{z},t)$ to the time-dependent fields $u(\mathbf{z},t)$. In particular, the force-force correlator $\Delta(u)$ that plays an essential role is related to the average

$$\Upsilon \equiv \overline{\langle \big[w(\mathbf{z},t) - w(\mathbf{z},t')\big]^2 \rangle} \tag{94}$$

over the random pinning forces and, at positive temperature, thermal noise. In general, Υ is a *functional* of $u(\mathbf{z},\tau)$ over all times τ. For zero temperature depinning, the case of primary interest, the possible fields u are limited to those that are non-decreasing in time. In this case, it can be seen that the crucial parts of Υ (which are sufficient to analyze the depinning critical behavior) depend only on $u(\mathbf{z},t) - u(\mathbf{z},t')$ and the functional Υ simplifies to a function of this one variable: it is then of the form assumed for $\Delta(u)$. In particular, if u does not change between t and t', w will not change either unless the w at the earlier time was the cause of a jump out of a formerly stable configuration into another; this jumping case can be handled by putting in time delays into the definition of u and, beyond this, the local dynamics will be independent on the history of u prior to times t and t'.

As soon as one considers a more general dynamics — e.g., still fluctuationless but with the applied force allowed to decrease with time, non-monotonic stress transfer kernels, or thermal noise — the simplification of the functional Υ does not occur. In general, it is then not clear how to proceed. In the case of interest for the present paper, one could first assume, as in all expansions about a mean field theory, that the fields are slowly varying in space and time and weakly fluctuating about a uniformly advancing solution which has a slow mean velocity v. The local displacements will lag behind due to the pinning but will be pulled ahead by the driving force: the balance of these effects determines the velocity–force relation. With thermal fluctuations, the displacements will lag less than they would otherwise because at low velocities they have the time to surmount energy barriers. Consider now the effects of a time dependent change in $u(\mathbf{z},t)$ on $\overline{\langle w(\mathbf{z},t)\rangle}$. If this change is very slow, w will follow approximately adiabatically. But if the change is relatively fast — as it can be due to the fast motion of a neighboring segment over a barrier — how the local displacement w will respond will depend crucially on whether it has already been near a surmountable barrier for some time, and thus is likely to have already surmounted it, or has recently arrived near a barrier and could thus be pushed over it by the change in u. Thus we expect the responses and correlations of w to depend on the whole prior (and intervening) history of the fields u.

The basic issue that must be addressed to make further progress is whether or not the essential information about the basic activation processes can be subsumed in simplified functions, such as the force-force correlator $\Delta(u-u')$, that appear in the formulation used in the present paper (note, however, that as we are performing an epsilon expansion, the central limit theorem is likely to be helpful: as we go from one scale to another, we can always assume that there is a large number of segments (or effective intermediate scale segments) whose dynamics contributes to the fields on larger scales). One possible route to proceed is to start by considering the nature of the typical fields that will arise from the thermally activated motion of large segments on the dynamics at smaller scales and ask whether the local responses to these are typically simple enough to be captured by the type of approximations used here.

We leave further work on these points as a challenge for the future. It is worth noting, however, that the physical origin of the problems, the intrinsic history dependence of the phenomena of interest, arise in many other non-equilibrium systems with many degrees of freedom. Better understanding of them in this context is thus likely to bear fruit more generally.

C. Alternative Expansions

Many of the difficulties encountered in this paper would be lessened if the energy scale — and hence the barriers — did not grow rapidly with length scale. One way to get around this difficulty might be to consider an expansion about a different limit, one in which not only the roughness exponent ζ is small, but also the scaling exponent θ for the energy. In d-dimensional manifolds with long range elastic interactions that fall off as $1/r^{d+\alpha}$ with $0 < \alpha < 2$, the upper critical dimension for both fluctuationless depinning and rough manifolds in equilibrium is $d_c = 2\alpha$ (i.e., $\zeta = 0$ at $d = d_c$). The energy scaling exponent is $\theta = d - \alpha + 2\zeta$ so that for α small, $\theta(d_c) = \alpha$ is also small. One might then hope to attempt an expansion in α and $\epsilon = d_c - d$ simultaneously. This would have the advantage that, assuming the barrier scaling exponent ψ is also small for small α near d_c, the exponential dependence of the velocity on the length dependent barriers would be relatively weak and hence, perhaps, systematically controllable. We must also leave this and other possible limits about which more controllable expansions might be attempted for future research.

D. Quasiclassical Langevin Equation

In addition to potential problems with the renormalization group formulation that are analogous to those discussed above for classical creep, in order to obtain results for quantum creep we have resorted to a quantum Langevin equation to approximate the quantum dynamics. We would like to be able to investigate this formalism more deeply and understand its limitations and regimes of validity. It is instructive to first consider simpler problems.

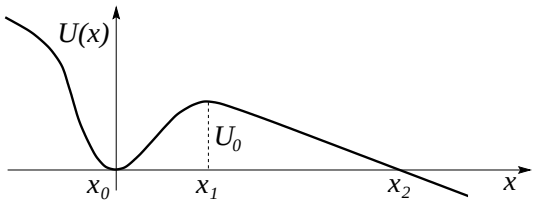

FIG. 5. Tunneling of an overdamped particle out of a 1D potential well in the presence of an external force f. The quantum mechanical answer for the tunneling action is of the form $S \propto 1/f^2$, $f \to 0$. The action obtained via the QLE is determined only by the region $x_0 < x < x_1$. Since $x_1 - x_0 \ll x_2 - x_1$, the QLE overestimates tunneling effects (i.e. gives smaller action).

The QLE can be used to analyze tunneling of a single particle if the barrier separating the metastable state from the lower-energy stable one has a single characteristic height and width. In this case the tunneling action obtained from the QLE differs from the true one only by a factor of order unity. In principle, the QLE can lead to an overestimation of the tunneling rate. For example, consider an overdamped particle (with viscosity η) in a 1D potential well $U(x)$ of depth U_0 with a minimum at $x = 0$ and $U(x)$ rapidly decaying for $x \to \pm\infty$. In the presence of an external force f, see Fig. 5, the well becomes metastable and the particle will leave. The quantum action S can be estimated as

$$S \simeq \eta(x_2 - x_1)^2 \approx \eta(U_0/f)^2. \tag{95}$$

This action is dominated by a region of width $\sim 1/f$ where the potential $U(x)$ is negligible but fx is less than the depth of the well: this yields $S \propto 1/f^2$ as $f \to 0$. If we use the QLE approximation, the tunneling action would be

much smaller than the true WKB value in the limit $f \to 0$: since the QLE is a *local* approximation, the only relevant part of the potential would be that for $x < x_1$, with x_1 the point where $U(x) - fx$ is maximal. In the QLE, once the random force that obeys the quantum fluctuation–dissipation theorem brings the particle to the point x_1, the particle can leave the well and the region $x > x_1$ that dominated the WKB action does not matter. Since in the limit $f \to 0$, $x_1 - x_0 \ll x_2 - x_1$, the tunneling action obtained within such an approach is much smaller than the correct one, $S_{QLE} \simeq \eta(x_1 - x_0)^2 \ll S$; the QLE can thus drastically *overestimate* tunneling rates.

We believe, however, that for the quantum creep problem considered in this paper the QLE should be a reasonably accurate approximation for the action whose exponential determines the velocity (81): in the naive scaling arguments, the effective potential wells that segments must tunnel out of have only one characteristic width and height. Nevertheless, the results we obtain from the QLE and RG analysis yield a much larger effective action for the tunneling than the naive scaling arguments. The source of this is unlikely to be due to the QLE approximation as, by analogy with the single particle case above, we would expect that, if anything, then the QLE would underestimate the tunneling action. This argument is reinforced by noting that the scaling analysis in section III can be applied directly to a system driven by a stochastic force obeying the quantum FDT for which the QLE is exact: these would lead to the same results as those obtained from the scaling arguments for the full quantum dynamical problem, see also Ref. 26.

VI. CONCLUSIONS

In this paper we have considered the motion of an elastic manifold driven through a disordered medium at low temperatures where quantum fluctuations are important. We have focused on the limit of small driving forces ($f \ll f_c$) for which the average velocity of the manifold is small and dominated by quantum tunneling through barriers between locally stable configurations. Using an at-least-partially controlled RG expansion, we find that the resulting creep velocity is exponentially small in a power of $1/f$. While for strong dissipation we find an intermediate range of forces where the creep law agrees with the result of simple scaling estimates (up to logarithmic corrections, cf. (17) and (83)), we find that the results of the RG analysis are more complex. In particular, at asymptotically small forces the creep velocity has the non-trivial form (81), combining an underlying massive (or other high-frequency) dynamics with an unexpected non-Arrhenius-like dependence on $\hbar$. The structure of the renormalization group flow is rather subtle and very different from that for classical creep. In particular, because of the importance of both rapid motion during a tunneling event and the slow overall motion, it is necessary to consider the dynamics of the manifold at *all* frequencies ω. This is in contrast to the classical case for which Chauve *et al.*[12] considered only the low-frequency limit of the dynamics. In the quantum case such a low-frequency approximation would lead to a spurious "localization transition" with the average velocity of the manifold dropping to zero at a small but finite value of the driving force. Although future improvements based on the analysis of the complete quantum mechanical action (9) rather than the quantum Langevin approximation might change some of the results presented here, we believe that the main feature, the importance of the whole spectrum of frequencies for the tunneling dynamics, will persist.

In spite of the subtleties that appeared in the analysis we have carried out there are further difficulties associated with both the broad distribution of barriers and the underlying field theoretic formulation of expansions about mean field theory. Although we have not resolved all the difficulties, and thus are not sure whether the present results are truly systematic, we have noted the physical and formal sources of the problems in ways that we hope will help direct future progress.

ACKNOWLEDGMENTS

DSF thanks L. Radzihovsky and L. Balents for the collaboration that led to the understanding of some of the subtleties in the RG scheme discussed in the last section. We thank J.-P. Bouchaud and D.R. Nelson for helpful discussions. This work was supported by the National Science Foundation under grants DMR 9976621, DMR 9809363, and DMR 9714725. We thank the Swiss National Science Foundation for financial support.

APPENDIX A: DERIVATION OF THE REAL-TIME QUANTUM ACTION

In this appendix we discuss the derivation of the action (9): Consider the *classical* equation of motion (4) with the δ-correlated noise $f_{\rm th}(\mathbf{z}, t)$; we search for the quantum Hamiltonian that reproduces the same equation of motion in the classical limit. One class of possible Hamiltonians has been introduced by Caldeira and Leggett[23] where the

system under consideration (an elastic manifold in our case) is assumed to be coupled to a bath consisting of harmonic oscillators. The Hamiltonian of the bath can be written in the form

$$\hat{H}_{\rm bath} = \int d^d z \sum_j \left[\frac{\hat{P}_j^2(\mathbf{z})}{2M_j(\mathbf{z})} + \frac{M_j(\mathbf{z})}{2}\Omega_j^2(\mathbf{z})\left(X_j(\mathbf{z}) - \frac{c_j(\mathbf{z})}{M_j(\mathbf{z})\Omega_j^2(\mathbf{z})}u(\mathbf{z})\right)^2\right], \tag{A1}$$

where each segment of the manifold $\mathbf{z}$ is coupled to the system of harmonic oscillators. This Hamiltonian contributes to the quantum-mechanical action with

$$\begin{aligned} S_{\rm bath}[\mathbf{X}] + S_{\rm int}[u,\mathbf{X}] = \int dt \int d^d z \sum_j \Bigg[& \frac{M_j(\mathbf{z})}{2}\dot{X}_j^2(\mathbf{z}) \\ & - \frac{M_j(\mathbf{z})}{2}\Omega_j^2(\mathbf{z})\left(X_j(\mathbf{z}) - \frac{c_j(\mathbf{z})}{M_j(\mathbf{z})\Omega_j^2(\mathbf{z})}u(\mathbf{z})\right)^2\Bigg], \end{aligned} \tag{A2}$$

where $\mathbf{X}$ is the vector with components X_j describing the oscillators of the bath. The action corresponding to the elastic manifold $S_0[u]$ has the form

$$S_0[u] = -\int dt \int d^d z \left[\frac{c}{2}\left(\frac{\partial u}{\partial \mathbf{z}}\right)^2 - \frac{\rho}{2}\left(\frac{\partial u}{\partial t}\right)^2 + U(u,\mathbf{z}) - fu\right]. \tag{A3}$$

After substituting the action $S = S_{\rm bath} + S_{\rm int} + S_0$ into Eq. (8) we can eliminate the bath degrees of freedom appearing only quadratically in the action. We define the spectral density

$$J(\omega) \equiv \frac{\pi}{2}\sum_j \frac{c_j^2(\mathbf{z})}{M_j(\mathbf{z})\Omega_j(\mathbf{z})}\delta(\omega - \Omega_j), \quad \omega > 0; \tag{A4}$$

the ohmic kernel $J(\omega) = \eta\omega$ produces the action (9). In the classical limit (high temperatures) one can *rigorously* expand the potential energy terms in (9) in $\tilde{y}$ and obtain the action (7) which is equivalent to Eq. (4). Note that we have introduced new coordinates $\tilde{u}$ and $\tilde{y}$ in the action (9) corresponding to the "center of mass" and relative motion of the trajectories in (8).

APPENDIX B: FIXED-POINT FUNCTION OF THE CORRELATOR

In this appendix we derive the relation (56). We investigate the static RG fixed-point in the absence of a driving force; the temperature and quantum fluctuations renormalize to zero, $C_l^>(\Lambda, t=0) \to 0$, and hence we need to consider the function $\Delta_l(u)$ alone. For $l < l_c$ we can neglect the nonlinear terms on the right-hand side of (28). Solving the remaining linear equation we obtain

$$\Delta_{l_c} \sim \Delta(0) e^{(\epsilon - 2\zeta)l_c} \tag{B1}$$

for the correlator height and $\xi^* \approx \xi \exp(-\zeta l_c)$ for its width (the latter result follows from integration of the second term in (28)). On the other hand, for $l \gg l_c$ the correlator is close to its fixed-point value. Using equation (28) for $\partial_l \Delta_l(u) = 0$ and substituting $u = 0$ we obtain

$$(\epsilon - 2\zeta)\,\Delta_{l_c}(0) \sim (\epsilon - 2\zeta)\,\Delta^*(0) \sim I{\Delta^{*\prime}}^2(+0) \tag{B2}$$

and replacing $I = A_d\Lambda^d/c^2\Lambda^4$ and $\zeta \sim \epsilon$ we obtain (56). Combining these results with $|\Delta^{*\prime}(0+)| \sim \Delta^*(0)/\xi^*$ we find the estimates $\Delta^*(0) \sim (c\Lambda^2)^2\xi^2\Lambda^{-d}e^{-2\zeta l_c}$ and $|\Delta^{*\prime}(0+)| \sim (c\Lambda^2)^2\xi\Lambda^{-d}e^{-\zeta l_c}$.

APPENDIX C: DANGEROUS RELEVANT VARIABLES

As mentioned in section V A, the RG flow generates dangerous *relevant* variables corresponding to the cumulants of the friction distribution[41]. From a physical point of view, the friction coefficient η in the equation of motion (4) is always spatially inhomogeneous due to the presence of disorder, so that the bare values of the cumulants describing the friction distribution are always nonzero. It turns out that under the RG transformation these cumulants grow

extremely rapidly and the description of the thermally activated or quantum motion in terms of the renormalized viscosity η_l or the function $D_l(\omega)$ (see section IV D) alone is not appropriate. Since the renormalized viscosity on a certain lengthscale corresponds to the waiting time on this scale, we conclude that the broad distribution of the friction (it is broad as the cumulants grow very rapidly) implies a broad distribution of waiting times. Hence, the proper description of the problem requires renormalization of the waiting time probability distribution function rather than its first moment alone. The main goal of this appendix is to show how the dangerous variables are renormalized under the RG flow. We will also show that even if initially all of them are zero, they will be generated by the random pinning. We will restrict ourselves to the case of high temperatures; the same variables will be generated in the quantum case.

Let us assume that the friction η in the equation of motion (4) is a spatially inhomogeneous function of the coordinate; in general, $\eta = \eta(u, \mathbf{z})$. For simplicity, we neglect the dependence on u (this does not change the result qualitatively). A physical realization where this approximation is valid is the pinned charge-density-wave: the friction $\eta(u, \mathbf{z})$ is a periodic function of u and, hence, can be expanded in a Fourier series; $\eta(\mathbf{z})$ then is the u-independent (the zeroth) harmonic. Below we will assume that the η-disorder and the Δ-disorder are uncorrelated and short-ranged; in reality, these two types of disorder should be correlated. If we take these correlations into account, the dangerous variables will still exist and the RG flow will be similar. In this section we assume that the response function has the form $1/\left(c\mathbf{k}^2 - i\eta_l\omega\right)$, i.e., we do not consider the full dynamic response associated with $D_l(\omega)$; this approach is valid in the classical case, see sections IV C and IV F.

Averaging over the disorder in η within the MSR-functional (7) we see that the friction term will be transformed into

$$\begin{aligned} &-\int d^dz dt\ \eta\dot{u}(\mathbf{z},t) iy(\mathbf{z},t) \to -\int d^dz dt\ \eta\dot{u}(\mathbf{z},t) iy(\mathbf{z},t) + A_{\rm rand} \\ &\equiv -\int d^dz dt\ \eta\dot{u}(\mathbf{z},t) iy(\mathbf{z},t) + \sum_{k\geq 2} A^{(k)} \\ &= -\int d^dz dt\ \eta\dot{u}(\mathbf{z},t) iy(\mathbf{z},t) + \sum_{k\geq 2} (-1)^k \eta^{(k)} \int d^dz \prod_{i=1}^{k} dt_i \dot{u}(\mathbf{z},t_i) iy(\mathbf{z},t_i). \end{aligned} \tag{C1}$$

When deriving the RG equations we consider the term $A_{\rm rand}$ and the usual disorder-induced term

$$A_{\rm dis} = \frac{1}{2}\int d^dz d\tau_1 d\tau_2\, \Delta\left[u(\mathbf{z},\tau_1) - u(\mathbf{z},\tau_2)\right] \tag{C2}$$

as perturbations. To one-loop order we have to calculate the second cumulant of the perturbation. There will be a cross-term of the form $\delta\langle A_{\rm rand} A_{\rm dis}\rangle_>$, where $\delta\langle H\rangle_>$ denotes the change in H after averaging over fast modes. Let us show that the average of this form gives rise to the singular renormalization of the coefficients $\eta^{(n)}$. Figure 6 summarizes the various symbols appearing in the diagrammatic expansion: Lines without arrows denote displacement fields u, lines with arrows at the end correspond to the auxiliary fields iy, and lines with arrows in the middle denote response functions. Crosses stand for time derivatives and the wavy horizontal lines denote disorder correlators $\Delta_l\left[u(\mathbf{z},t_1) - u(\mathbf{z},t_2)\right]$. Dashed horizontal lines stand for $(-1)^k\eta^{(k)}$ and dots ... represent further omitted lines. For each response function with an arrow coming into a wavy vertex (see e.g., the diagrams in Figs. 8(a) and (b)), the disorder correlator $\Delta[u(\mathbf{z},t_1) - u(\mathbf{z},t_2)]$ is differentiated with respect to its argument. These derivatives appear as a consequence of averaging of the correlator and the iy-fields, see Eq. (C4) below. Dashed and wavy lines in diagrams connect times, the upper line connects t_1, t_2, ..., and the lower line connects the times τ_1 and τ_2. Note that there is no time ordering corresponding to vertical or horizontal directions. The fields at the upper vertices in diagrams are taken at the spacial coordinate $\mathbf{z}$ and the lower vertex is at $\mathbf{z}'$. The argument of the response function involves the differences between the times and spatial coordinates of the end and starting points. We quote three useful formulae

$$\delta\langle u(\mathbf{z},t) iy(\mathbf{z}',t')\rangle_> = R_l^>(\mathbf{z}-\mathbf{z}', t-t')dl \tag{C3}$$

$$\delta\left\langle \Delta\left[u(\mathbf{z},\tau_1) - u(\mathbf{z},\tau_2)\right] iy(\mathbf{z}',t')\right\rangle_> = \Delta'\left[u(\mathbf{z},\tau_1) - u(\mathbf{z},\tau_2)\right]\left[R_l^>(\mathbf{z}-\mathbf{z}',\tau_1-t') - R_l^>(\mathbf{z}-\mathbf{z}',\tau_2-t')\right]dl \tag{C4}$$

$$\int d^dz' R_l^>(\mathbf{z}',t_1) R_l^>(\mathbf{z}',t_2) = \frac{A_d\Lambda^d}{(2\pi)^d}\, dl\, R_l(\Lambda,t_1) R_l(\Lambda,t_2), \tag{C5}$$

where $R_l(\Lambda,t)$ denotes the (partly Fourier transformed) response function (25) and $R_l^>(\Lambda,t)$ is defined in (36).

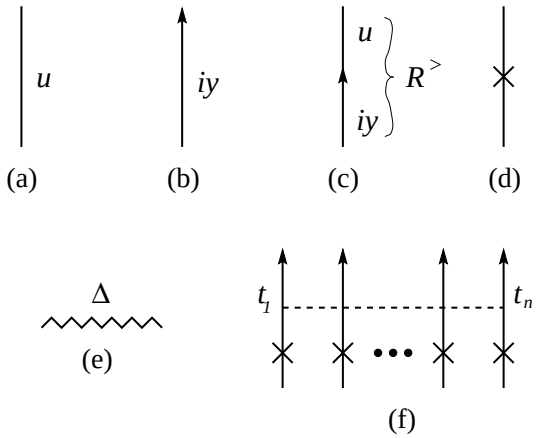

FIG. 6. Elements used in diagrams: (a) the displacement field u; (b) the iy-field; (c) the response function $R^{>}$; (d) crosses denote derivatives, with respect to time in the u-field if the cross is on a solid line, or with respect to the time difference in the response function if the cross is on a response function line; (e) diagrammatic representation of the correlator Δ; (f) diagrammatic representation of random friction terms $(-1)^n\eta^{(n)}\prod\dot{u}(\mathbf{z},t_k)iy(\mathbf{z},t_k)$, see (C1); dots ... stand for further omitted lines.

The contribution δD_1 of the diagram in Fig. 7(a) has the form,

$$\delta D_1 = \frac{1}{2}\eta_l^{(n)}\int d^dz d^dz' \int d\tau_1 d\tau_2 \left[\prod_{k=1}^{n} dt_k\right] \delta\left\langle \dot{u}(\mathbf{z},t_1) iy(\mathbf{z}',\tau_1)\right\rangle_{>} \delta\left\langle \dot{u}(\mathbf{z},t_2) iy(\mathbf{z}',\tau_2)\right\rangle_{>}$$
$$\times iy(\mathbf{z},t_1) iy(\mathbf{z},t_2)\Delta_l\left[u\left(\mathbf{z}',\tau_1\right)-u\left(\mathbf{z}',\tau_2\right)\right]\prod_{k=3}^{n}\dot{u}(\mathbf{z},t_k)iy(\mathbf{z},t_k) \qquad \text{(C6)}$$
$$= \frac{1}{2}\eta_l^{(n)}\frac{A_d\Lambda^d}{(2\pi)^d}dl\int d^dz\left[\prod_{k=1}^{n}dt_k\right]\dot{R}_l(\Lambda,t_1-\tau_1)\dot{R}_l(\Lambda,t_2-\tau_2)iy(\mathbf{z},t_1)iy(\mathbf{z},t_2)$$
$$\times\int d\tau_1 d\tau_2\,\Delta_l\left[u\left(\mathbf{z},\tau_1\right)-u\left(\mathbf{z},\tau_2\right)\right]\prod_{k=3}^{n}\dot{u}(\mathbf{z},t_k)iy(\mathbf{z},t_k).$$

In the last equation, we have used (C3) in order to express averages over fast modes through response functions and have integrated over $\mathbf{z}'$ using (C5). We rewrite the product of the two response functions as $\dot{R}_l(\Lambda,t_1-\tau_1)\dot{R}_l(\Lambda,t_2-\tau_2) = \partial_{\tau_1}R_l(\Lambda,t_1-\tau_1)\partial_{\tau_2}R_l(\Lambda,t_2-\tau_2)$ and integrate by parts over variables τ_1 and τ_2, thus generating the second derivative of the correlator Δ. The response functions connect times t_1 and τ_1 and t_2 and τ_2. Consequently, we can set $t_1\approx\tau_1$ and $t_2\approx\tau_2$ in the time arguments of the iy-fields and integrate over the variables t_1 and t_2 in the response functions using the formula $\int dtR(\Lambda,t) = R(\Lambda,\omega=0) = 1/c\Lambda^2$. In the end we obtain an expression involving the integrals $\int d^dz\,d\tau_1\,d\tau_2\,dt_3\ldots dt_n$ and performing substitution $\tau_1\to t_1$ and $\tau_2\to t_2$ we arrive at the final contribution of the diagram 7(a)

$$\delta D_1 = -\frac{1}{2}\eta_l^{(n)}\frac{A_d\Lambda^d}{(2\pi)^d}\frac{dl}{\left(c\Lambda^2\right)^2}\int d^dz\left[\prod_{k=1}^{n}dt_k\dot{u}(\mathbf{z},t_k)iy(\mathbf{z},t_k)\right]\Delta_l'\left[u\left(\mathbf{z},t_1\right)-u\left(\mathbf{z},t_2\right)\right]. \qquad \text{(C7)}$$

Note that in the diagrammatic language integrating by parts corresponds to drawing u-field lines out of the wavy vertex and moving crosses (i.e., time-derivatives) from the response functions down to the displacement fields. The low-frequency expansion of the diagram in Fig. 7(a) then takes the form of the diagram in Fig. 6(f) [this low-frequency analysis involves the expansion of the argument $u(\mathbf{z},\tau_1)-u(\mathbf{z},\tau_2)$ of the correlator Δ in a Taylor series in powers of $(\tau_1-\tau_2)$; the first term (equal to zero) of this expansion produces the desired contribution]. There are $n(n-1)$ equivalent diagrams of the type in Fig. 7(a) allowed by the permutation symmetry.

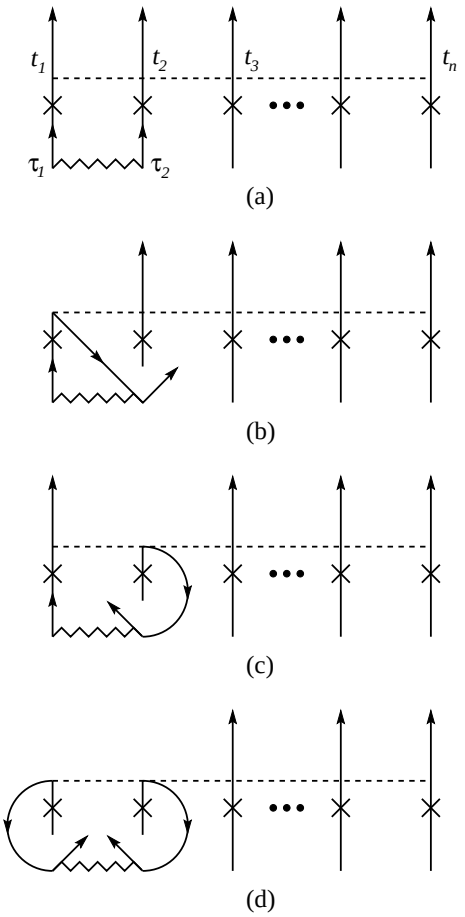

FIG. 7. Dangerous diagrams contributing to the renormalization of the cumulants of the friction-coefficient distribution. These terms arise from averaging over fast modes in $\langle A_{\rm rand} A_{\rm dis}\rangle_>$: (a) with multiplicative factors $n(n-1)$ (due to the permutation symmetry), (b) with multiplicative factor $2n$, (c) with multiplicative factor $2n(n-1)$, (d) with multiplicative factor $n(n-1)/2$. For convenience we draw some of the iy-fields and response functions at a 45 degrees angle or deform the lines.

The expression corresponding to the diagram in Fig. 7(b) is given by

$$\begin{aligned}\delta D_2 = \frac{1}{2}\eta_l^{(n)} \int d^d z d^d z' \int d\tau_1 d\tau_2 \left[\prod_{k=1}^{n} dt_k\right] \delta\langle \dot{u}(\mathbf{z},t_1) iy(\mathbf{z}',\tau_1)\rangle_> \delta\langle \Delta_l\left[u\left(\mathbf{z}',\tau_1\right) - u\left(\mathbf{z}',\tau_2\right)\right] iy(\mathbf{z},t_1)\rangle_> \\ \times iy(\mathbf{z}',\tau_2) \prod_{k=2}^{n} \dot{u}(\mathbf{z},t_k) iy(\mathbf{z},t_k) \qquad\qquad (C8) \\ = -\frac{1}{2}\eta_l^{(n)} \Delta_l''(0) \frac{A_d \Lambda^d}{(2\pi)^d} \frac{dl}{(c\Lambda^2)^2} \int d^d z \prod_{k=1}^{n} dt_k \dot{u}(\mathbf{z},t_k) iy(\mathbf{z},t_k);\end{aligned}$$

there are $2n$ topologically equivalent diagrams of this class. Note that in contrast to the term δD_1 the argument of the function $\Delta_l(u)$ in the above expression is zero. The diagram shown in Fig. 7(c) gives the contribution

$$\begin{aligned}\delta D_3 = \frac{1}{2}\eta_l^{(n)} \int d^d z d^d z' \int d\tau_1 d\tau_2 \left[\prod_{k=1}^{n} dt_k\right] \delta\langle \dot{u}(\mathbf{z},t_1) iy(\mathbf{z}',\tau_1)\rangle_> \delta\langle \Delta\left[u\left(\mathbf{z}',\tau_1\right) - u\left(\mathbf{z}',\tau_2\right)\right] iy(\mathbf{z},t_2)\rangle_> \\ \times iy(\mathbf{z},t_1)\dot{u}(\mathbf{z},t_2) iy(\mathbf{z}',\tau_2) \prod_{k=3}^{n} \dot{u}(\mathbf{z},t_k) iy(\mathbf{z},t_k) \qquad\qquad (C9) \\ = -\frac{1}{2}\eta_l^{(n)} \frac{A_d \Lambda^d}{(2\pi)^d} \frac{dl}{(c\Lambda^2)^2} \int d^d z \left[\prod_{k=1}^{n} dt_k \dot{u}(\mathbf{z},t_k) iy(\mathbf{z},t_k)\right] \Delta_l''\left[u\left(\mathbf{z},t_1\right) - u\left(\mathbf{z},t_2\right)\right];\end{aligned}$$

there are $2n(n-1)$ topologically equivalent diagrams of this class. Finally, the diagram in Fig. 7(d) is given by the expression

$$\delta D_4 = \frac{1}{2}\eta_l^{(n)} \int d^d z d^d z' \int d\tau_1 d\tau_2 \left[\prod_{k=1}^{n} dt_k\right] \dot{u}(\mathbf{z},t_1)\dot{u}(\mathbf{z},t_2) iy(\mathbf{z}',\tau_1) iy(\mathbf{z}',\tau_2)$$
$$\times \left[\prod_{k=3}^{n} \dot{u}(\mathbf{z},t_k) iy(\mathbf{z},t_k)\right] \delta\left\langle iy(\mathbf{z},t_1)\delta\left\langle \Delta\left[u\left(\mathbf{z}',\tau_1\right) - u\left(\mathbf{z}',\tau_2\right)\right] iy(\mathbf{z},t_2)\right\rangle_{>}\right\rangle_{>}$$
$$= \frac{1}{2}\eta_l^{(n)} \frac{A_d\Lambda^d}{(2\pi)^d}\frac{dl}{\left(c\Lambda^2\right)^2} \int d^d z \left[\prod_{k=1}^{n} dt_k\right] d\tau_1 d\tau_2 \dot{u}(\mathbf{z},t_1)\dot{u}(\mathbf{z},t_2) iy(\mathbf{z},\tau_1) iy(\mathbf{z},\tau_2) \left[\prod_{k=3}^{n} \dot{u}(\mathbf{z},t_k) iy(\mathbf{z},t_k)\right]$$
$$\times \{R(\Lambda,\tau_1-t_1)R(\Lambda,\tau_1-t_2) + R(\Lambda,\tau_2-t_1)R(\Lambda,\tau_2-t_2)$$
$$-R(\Lambda,\tau_1-t_1)R(\Lambda,\tau_2-t_2) - R(\Lambda,\tau_1-t_2)R(\Lambda,\tau_2-t_1)\}\Delta''\left[u\left(\mathbf{z},\tau_1\right) - u\left(\mathbf{z},\tau_2\right)\right] = 2\delta D_3. \tag{C10}$$

The first two terms in the curly brackets do not feed back to the random friction cumulants, while the third and fourth terms give the desired contribution. The multiplication factor of the diagram in Fig. 7(d) is equal to $n(n-1)/2$.

In order to find the contribution to $\eta_l^{(n)}$ we need to set the argument $u(\mathbf{z},t_1) - u(\mathbf{z},t_2)$ in the correlator $\Delta(u)$ to zero in (C7), (C9), and (C10) (as only this term feeds back to the random friction cumulants) and sum over the four contributions (C7), (C8), (C9), and (C10) each multiplied with its appropriate weight; the result takes the form

$$\delta\eta_l^{(n)} = -\eta_l^{(n)}\left(2n^2-n\right)\frac{A_d\Lambda^d}{(2\pi)^d}\frac{\Delta_l''(0)}{\left(c\Lambda^2\right)^2}dl. \tag{C11}$$

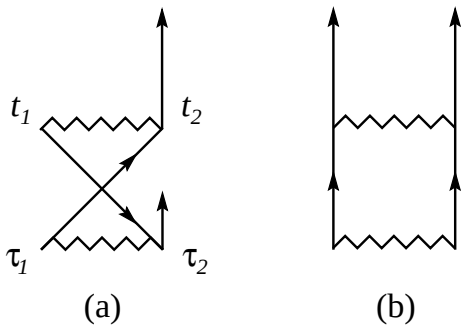

FIG. 8. Diagrams describing the generation of the second cumulant of the friction distribution; their low-frequency expansions feed back to the second cumulant.

Next, we show that the term $A_{\rm dis}$ itself generates the second cumulant $\eta^{(2)}$. The dangerous relevant diagrams arise from the average $\langle A_{\rm dis}A_{\rm dis}\rangle_{>}$, see Fig. 8; their low-frequency expansion gives the contribution to the random friction. The contribution of the diagram 8(a) takes the form

$$\delta\tilde{D}_1 = \frac{1}{8}\frac{A_d\Lambda^d}{(2\pi)^4}dl \int d^d z dt_1 dt_2\ \Delta_l'\left[u(\mathbf{z},t_1) - u(\mathbf{z},t_2)\right] iy(\mathbf{z},t_2) iy(\mathbf{z},\tau_2)$$
$$\times \int d\tau_1 d\tau_2\ \Delta_l'\left[u(\mathbf{z},\tau_1) - u(\mathbf{z},\tau_2)\right] R_l(\Lambda,t_2-\tau_1)R_l(\Lambda,\tau_2-t_1), \tag{C12}$$

where the averaging over fast modes and the integration over $\mathbf{z}'$ has already been carried out. The response functions connect the times $t_2,\ \tau_1$ and $\tau_2,\ t_1$ and we can expand

$$u(\mathbf{z},t_1) - u(\mathbf{z},t_2) = u(\mathbf{z},\tau_2 + (t_1-\tau_2)) - u(\mathbf{z},t_2)$$
$$\approx u(\mathbf{z},\tau_2) - u(\mathbf{z},t_2) + \dot{u}(\mathbf{z},\tau_2)(t_1-\tau_2); \tag{C13}$$

similarly, $u(\mathbf{z},\tau_1) - u(\mathbf{z},\tau_2) \approx u(\mathbf{z},t_2) - u(\mathbf{z},\tau_2) + \dot{u}(\mathbf{z},t_2)(\tau_1-t_2)$. Substituting these expansions into (C12) and expanding the correlators $\Delta'(u)$ we arrive at the expression (note that $\int dt\, tR(\Lambda,t) = \eta_l/\left(c\Lambda^2\right)^2$)

$$\delta\tilde{D}_1 = \frac{1}{8}\frac{A_d\Lambda^d}{(2\pi)^d}\frac{\eta_l^2}{(c\Lambda^2)^4}dl$$
$$\times \int d^dz dt_1 dt_2\, \Delta_l''^2\left[u(\mathbf{z},t_1)-u(\mathbf{z},t_2)\right]\dot{u}(\mathbf{z},t_1)iy(\mathbf{z},t_1)\dot{u}(\mathbf{z},t_2)iy(\mathbf{z},t_2); \tag{C14}$$

there are 4 topologically equivalent diagrams of this class.

Diagram (b) in Fig. 8 gives the contribution

$$\delta\tilde{D}_2 = \frac{1}{8}\frac{A_d\Lambda^d}{(2\pi)^d}dl\int d^dz dt_1 dt_2\, \Delta_l''\left[u(\mathbf{z},t_1)-u(\mathbf{z},t_1)\right]iy(\mathbf{z},t_1)iy(\mathbf{z},t_2)$$
$$\times \int d\tau_1 d\tau_2\, \Delta_l\left[u(\mathbf{z},\tau_1)-u(\mathbf{z},\tau_2)\right]R_l(\Lambda,\tau_1-t_1)R_l(\Lambda,\tau_2-t_2), \tag{C15}$$

where the averaging over fast modes and the integration over $\mathbf{z}'$ again has been performed already. The response functions connect the points τ_1 and t_1 and τ_2 and t_2. Expanding the displacement fields in $t_1-\tau_1$ and τ_2-t_2, substituting them into (C15), and expanding the correlator $\Delta(u)$ we see that $\delta\tilde{D}_2 = \delta\tilde{D}_1$. There are 4 topologically equivalent diagrams of class (b). Summing up the contributions $\delta\tilde{D}_1$ and $\delta\tilde{D}_2$ and multiplying the sum by 4 we obtain the contribution $\delta\tilde{\eta}_l^{(2)}$ of the disorder term to the second cumulant,

$$\delta\tilde{\eta}_l^{(2)} = \frac{A_d\Lambda^d}{(2\pi)^d}\frac{\eta_l^2}{(c\Lambda^2)^4}\Delta_l''^2(0)dl. \tag{C16}$$

Finally, we can write the one-loop RG equation for the cumulants of the random friction distribution; accounting for the terms (C7), (C8), (C9), (C10), and (C16) we find the flow equations

$$\partial_l\eta_l^{(2)} = (4-d-2z)\,\eta_l^{(2)} + I\frac{\eta_l^2}{(c\Lambda^2)^4}\Delta_l''^2(0) - \frac{6I}{(c\Lambda^2)^2}\Delta_l''(0)\eta_l^{(2)}, \tag{C17}$$

$$\partial_l\eta_l^{(n)} = (d+2n-dn-zn)\,\eta_l^{(n)} - \left(2n^2-n\right)\frac{I}{(c\Lambda^2)^4}\Delta_l''(0)\eta_l^{(n)}, \qquad n\neq 2. \tag{C18}$$

The system of RG equations (C17) and (C18) has been derived to lowest order in $4-\epsilon$. To next order, the second cumulant will generate the third cumulant. To third order, the third cumulant will generate the fourth cumulant, etc., i.e., *all* cumulants will be generated in the RG flow even if all of them (except for the first one) are equal to zero initially. From a physical point of view, the friction will always be random as the point-like impurities suppress the order parameter randomly and, hence, the dynamic characteristics of the medium (e.g., a superconductor) is random as well. Since $-\Delta_l''(0) \propto 1/T_l \propto e^{\theta l}$ and the correction due to disorder grows as n^2 for large n, the random friction probability distribution becomes very broad and one needs to take into account *all* its moments and not just the friction η_l only. In order to obtain Eqs. (C17) and (C18) we have made the approximation $u(\mathbf{z},t_1)-u(\mathbf{z},t_2)=0$ in the final expressions for δD_1, δD_3, $\delta\tilde{D}_1$, and $\delta\tilde{D}_2$; in general, however, one needs to renormalize the full functional (93). During the RG procedure, other terms will be generated and it is unclear at this stage how to take all these terms into account in a controllable way.

---

[1] G. Blatter *et al.*, Rev. Mod. Phys. **66**, 1125 (1994).
[2] G. Grüner, Rev. Mod. Phys. **60**, 1129 (1988).
[3] S. Lemerle, J. Ferré, C. Chappert, V. Mathet, T. Giamarchi, and P. Le Doussal, Phys. Rev. Lett. **80**, 849 (1998).
[4] D.S. Fisher, K. Dahmen, S. Ramanathan, and Y. Ben-Zion, Phys. Rev. Lett. 78, 4885 (1997)
[5] M. Mezard, cond-mat/9801029 and references therein.
[6] J. Krug, Adv. Phys. **46**, 139 (1997).
[7] J.G. Conlon *et al.*, Comm. Math. Phys. **116**, 417 (1988).
[8] M.V. Feigelman, V.B. Geshkenbein, A.I. Larkin, and V.M. Vinokur, Phys. Rev. Lett. **63**, 2303 (1989).
[9] M.P.A. Fisher, Phys. Rev. Lett. **62**, 1415 (1989).
[10] D.S. Fisher, M.P.A. Fisher, and D.A. Huse, Phys. Rev. B **43**, 130 (1991).

[11] L. Radzihovsky, "Equilibrium Dynamics of Pinned Periodic Media: Dynamic FRG", Bull. Am. Phys. Soc., E37.08 (1998), abstract available at http://www.aps.org/BAPSMAR98/abs/S1110008.html; based on Ref. 41.
[12] P. Chauve, T. Giamarchi, and P. Le Doussal, Europhys. Lett. **44**, 110 (1998); P. Chauve, T. Giamarchi, and P. Le Doussal, Phys. Rev. B **62**, 6241 (2000).
[13] S.N. Coppersmith, Phys. Rev. B, 2073 (1986).
[14] For a review see Y. Yeshurun, A.P. Malozemoff, and A. Shaulov, Rev. Mod. Phys. **68**, 911 (1996).
[15] J.A. Baldwin and F. Milstein, J. Appl. Phys. **45**, 4006 (1974).
[16] S.V. Zaitsev-Zlotov, Phys. Rev. Lett. **71**, 605 (1993).
[17] G. Blatter, V.B. Geshkenbein, and V.M. Vinokur, Phys. Rev. Lett. **66**, 3297 (1991).
[18] D.S. Fisher, Phys. Rev. Lett. **56**, 1964 (1986).
[19] P.C. Martin, E.D. Siggia, and H.A. Rose, Phys. Rev. A **8**, 423 (1973).
[20] H.K. Janssen, Z. Phys. **23**, 377 (1976).
[21] R.P. Feynman and A.R. Hibbs, *Quantum Mechanics and Path Integrals* (McGraw-Hill, New York, 1965).
[22] R.P. Feynman and F.L. Vernon, Jr, Ann. Phys. (N.Y.) **24**, 118 (1963).
[23] A.O. Caldeira and A.J. Leggett, Ann. Phys. (N.Y.) **149**, 374 (1983).
[24] see p. 274 in G. Schön and A.D. Zaikin, Phys. Rep. **198**, 237 (1990).
[25] A. Schmid, J. Low Temp. Phys. **49**, 609 (1982).
[26] U. Eckern, W. Lehr, A. Menzel–Dorwarth, F. Pelzer, and A. Schmid, J. Stat. Phys. **59**, 885 (1990).
[27] R.H. Koch, D.J. van Harlingen, and J. Clark, Phys. Rev. Lett. **45**, 2132 (1980).
[28] By colored noise we mean any stochastic force whose Fourier transform of the correlator is not a constant in the ω-space.
[29] D.S. Fisher, J. Appl. Phys. **61**, 3672 (1987).
[30] For three dimensional spin glasses, numerical evidence suggests $\theta \approx 0.2$, see see A. J. Bray and M. A. Moore, J. Phys. C **17**, L463 (1984) and W. L. McMillan, Phys. Rev. B **29**, 4026 (1984). The numerical calculation of the exponent Ψ governing the barriers gives $\Psi \approx 1.0$, see L Berthier and J. P. Bouchaud, cond-mat/0202069.
[31] M.P.A. Fisher and P. Young, Phys. Rev. Lett. **66**, 2931 (1991).
[32] S. Scheidl, Z. Phys. B **97**, 345 (1995); P. Le Doussal and V.M. Vinokur, Physica C **254**, 63 (1995); D.A. Gorokhov and G. Blatter, Phys. Rev. B **58**, 213 (1998).
[33] O. Narayan and D.S. Fisher, Phys. Rev. B **46**, 11520 (1992).
[34] O. Narayan and D.S. Fisher, Phys. Rev. B **48**, 7030 (1993).
[35] T. Nattermann, S. Stepanov, L.H. Tang, and H. Leschhorn, J. Phys. II **2**, 1483 (1992).
[36] M. Müller, D.A. Gorokhov, and G. Blatter, Phys. Rev. **63**, 184305 (2001).
[37] A.J. Leggett, S. Chakravarty, A.T. Dorsey, M.P.A. Fisher, A. Garg, and W. Zwerger, Rev. Mod. Phys. **59**, 1 (1987).
[38] L. Balents, Europhys. Lett. **24**, 489 (1993).
[39] Another open question is related to the solution of the RG equations in section IV B. ¿From the mathematical point of view it is not easy to describe the crossover from the regime $u_{\rm vel} \ll u_{\rm smear}$ to $u_{\rm vel} \gg u_{\rm smear}$. We expect that the behavior of the manifold on large scales $L \gg L_f$ will be nontrivial. In particular for the random bond disorder, the wandering exponent on scales $L \lesssim L_f$ and $L \gtrsim L_f$ will be different. This, however, will not affect the results for the velocity.
[40] L.D. Landau and E.M. Lifshitz, *Statistical Physics*, Course in Theoretical Physics Vol. 5 (Pergamon, London–Paris, 1958).
[41] L. Radzihovsky, L. Balents, and D.S. Fisher, unpublished.